PERFORMANCE OF GEOCELL SUPPORTED EMBANKMENT USING PLAXIS

MAJOR II PROJECT REPORT

SUBMITTED IN PARTIAL FULFILLMENT OF THE REQUIREMENTS

FOR THE AWARD OF THE DEGREE

OF

MASTERS OF TECHNOLOGY

IN

GEOTECHNICAL ENGINEERING

Submitted by:

AYESHA RASHID

2K18/GTE/05

Under the supervision of

PROF. A.K.SAHU

DEPARTMENT OF CIVIL ENGINEERING

DELHI TECHNOLOGICAL UNIVERSITY

(Formerly Delhi College of Engineering)

Bawana Road, Delhi-110042

JULY, 2020

DELHI TECHNOLOGICAL UNIVERSITY

(Formerly Delhi College of Engineering)

Bawana Road, Delhi-110042

CANDIDATE'S DECLARATION

I, **Ayesha Rashid, 2K18/GTE/05**, student of M.Tech, Geotechnical Engineering, hereby declare that the project dissertation titled "**Performance of geocell supported embankment using PLAXIS**" which is submitted by me to the Department of Civil Engineering, Delhi Technological University, Delhi in partial fulfillment of the requirements for the award of the degree of Master of Technology, is original and not copied from any source without proper citation. This work has not previously formed the basis for the award of any degree, diploma associateship, fellowship or other similar title or recognition.

Place: Delhi

Date: 10^{th} August2020 (AYESHA RASHID)

DEPARTMENT OF CIVIL ENGINEERING

DELHI TECHNOLOGICAL UNIVERSITY

(Formerly Delhi College of Engineering)

Bawana Road, Delhi – 110042

CERTIFICATE

I hereby certify that the Project Dissertation titled "**Performance of Geocell Supported Embankment Using PLAXIS**" which is submitted by Ayesha Rashid, 2K18/GTE/05, Department of Civil Engineering, Delhi Technological University, Delhi in partial fulfilment of the requirement for the award of the degree of Master of Technology, is a record of the project work carried out by the students under my supervision. To the best of my knowledge this work has not been submitted in part or full for any Degree or Diploma to this University or elsewhere.

Place: Delhi (**PROF. A.K.SAHU**)

Date: 10^{th} August 2020 SUPERVISOR

ACKNOWLEDGEMENTS

I express my profound gratitude and have no words to reveal my gratefulness to Prof. A.K.Sahu, Department of Civil Engineering, Delhi Technological University, Delhi, whose able guidance and provoking of encouragement has been the great force that enabled me to prepare this project report on the topic "**Performance of Geocell Supported Embankment Using PLAXIS** ". He devoted considerable time in guiding and checking my work and made valuable suggestions.

I am grateful to Prof. Yogesh Singh, Vice Chancellor and Prof. Nirendra Dev, Head of Civil Engineering Department for the facilities provided to carry on the work. I am thankful to all the faculty members of Geotechnical Engineering for their cooperation and moral support and to all those who helped me in making this project better by providing their valuable comments and guidance.

I would also like to thank my parents and lab assistants who helped me in performing the project work within the limited time frame.

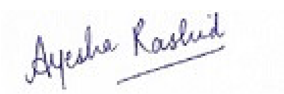

(AYESHA RASHID)
2K18/GTE/05

ABSTRACT

In this study, work on PLAXIS 2D software was carried out to study the performance of geocell supported embankment. Properties of uniaxial geogrids (UG), biaxial geogrids (BG) and two types of non-oriented high-density polyethylene geogrids- NG1 and NG2, used to form geocell mattress were considered for the study. The geocell reinforced layer of soil was simulated as equivalent soil layer by empirical equations. The heights of the geocell mattress made from BG geogrid was varied as 100mm, 125mm and 150mm to study the effect of height of the geocell in embankment stability. Apart from the height of the geocell mattress, in the case of the BG01 geocell layer, the infill material of geocell pockets was varied. Geocell openings filled with sandy soil gave better performance than when filled with clayey soil. The surcharge load on the embankment of 400mm height to obtain a factor of safety of 1.15 was calculated for different geometry and types of geocells. The depth and material of the geocell mattress affect the strength and deformation of the soil considerably. A design problem is discussed in detail to describe the analysis presented in this study.

CONTENTS

LIST OF TABLES

LIST OF FIGURES

LIST OF ABBREVATIONS

ABBREVATION	DESCRIPTION
c	Vane shear strength
d_e	Equivalent diameter of geocell
h	Height of geocell mattress
M	Secant modulus of geocell
$\Delta\sigma_3$	Additional confining strength due to geocell
C_r	Additional cohesion due to geocell
C_g	Cohesion strength of geocell layer
φ	Angle of internal friction
UG	Geocell made up of uniaxial geogrid
UG01	Geocell mattress of height 100 mm made up of uniaxial geogrid
BG	Geocell made up of biaxial geogrid
NP	Non-oriented high density polypropylene
BG01	Geocell mattress of height 100mm formed using biaxial geogrid
BG015	Geocell mattress of height 150mm formed using biaxial geogrid
BG02	Geocell mattress of height 200mm formed using biaxial geogrid
K_p	Coefficient of passive earth pressure
K_o	Coefficient of passive earth pressure
ε_a	Axial strain at failure
d_0	Initial diamteter of individual cell
E_g	Equivalent modulus of geocell encased soil
FEM	Finite element method
U_x	Horizontal displacement
U_y	Vertical displacement
Msf	Factor of safety

CHAPTER 1

INTRODUCTION

1.1 GENERAL

In geotechnical engineering, soil stabilization has most commonly be done by adding chemicals that have resulted in many environmental issues, like large CO_2 emission, natural resource depletion and dust generation (Van Deventer et al., 2010). On the other hand, geosynthetics like geotextiles, geonets, geocomposites, geomembranes, geogrids, reduce the harmful impact on the environment since there is no requirement of natural resources for its manufacturing. The geosynthetics are manufactured in factories; therefore, the quality control is easy. Among the different types of geosynthetics, geocells are comparatively a new material and offer greater advantages over the other conventional geosynthetics.

Geocell provides 3-dimensional confinement to the soil. It is an interconnected network of cells prepared from polymeric materials. The geocells mattresses are manufactured at factories, delivered at the field, laid by expanding the mattress on the ground, and then the cells are filled with soil or aggregates. During the vertical application of load on geocells, the active earth pressure, which depends on frictional resistance generated between the soil-filled in geocell and the geocell walls, gets mobilized. This provides higher engineering strength and durability to the structure reinforced with geocells. Geocells are economical as it does not require any maintenance.

OBJECTIVE OF THE STUDY

The objective of the study is to understand the performance of geocell reinforced embankment in PLAXIS 2D by varying:

1. Depth of geocell mattress
2. Material of the geocell mattress, and
3. Infill material of geocell pockets.

The surcharge load has been calculated for different types of geocells- UG, BG01, BG015, BG02, BG01 (clay), NG1 and NG2- to obtain a factor of safety of 1.15. The characteristics of geocells- height and secant modulus of geocell, and type of soil for filling the geocell openings, are sensitive criteria for determining the performance of geocell reinforced embankment and have been analyzed in detail.

CHAPTER 2

LITERATURE REVIEW

2.1. GENERAL

Use of geosynthetics in geotechnical engineering for encountering problems related to slope stability, retaining walls, road bases, embankment construction, channel linings have been in practice for some time now. Geosynthetics like geogrids, geonets, geomembranes, etc are planar reinforcement and provide confinement in two directions only. While geocells provide confinement in three dimensions.

2.2 LITERATURE REVIEW

Different authors have carried out researches on the geocell application in the construction field. Geocells provide confinement to the soil and enhance the bearing capacity of the soil reducing the risk of failure due to large settlement. The dispersion of load mechanism and confinement effect has been analyzed in a study (Avesani et al. 2013). A new method was proposed taking into consideration the geometry of geocells, geocell in-fill soil, foundation soil and type of loading. The experimental results showed similarity with other methods in practice such as Presto's method and Koerner's method. The results were analyzed for both sandy and clayey soil.

A. M. Hegde and Sitharam (2015) conducted experimental tests to study the impact of infill material on geocell behavior. The increase in strength of the geocell bed increased by 12 folds, 10 folds and 9 folds for aggregate infill, sand infill and red soil infill, respectively. All three infill decreased the settlement marginally. The settlement for the case of aggregate was least. The study also showed that the composite reinforcement of basal geogrid and geocell prevented the surface heaving of the soil for all the infill material used.

Dash et al. (2007) researched the provision of geocell reinforcement in sand beds. The model was prepared in the laboratory. The load was applied in the form of strip footing. Characteristics of geocells- height and width of the geocell mattress, geocell formation pattern- triangular, chevron, diamond, pocket-size of geocell, stiffness of the material used for geocell fabrication and infill material in geocell pockets, influence on bearing capacity and settlement of sand was determined. Another study showed improvement when a planar reinforcement was done in addition to the geocell reinforcement at appropriate depths (Dash et. al 2001). In a similar study, the load was applied in the form of circular footing Application of geocells in the sand layer increased the bearing capacity and reduced the surface heaving of the foundation bed significantly (Dash et al., 2003).

Han et al. (2008) studied the behavior of soil reinforced with geocell by experimental and numerical studies. The confinement provided by the 3-D structure of geocells increased the bearing capacity along with the elastic modulus of the foundation soil. The joints in the geocell should have sufficient strength. For the deformation of 1.25mm, the load-carrying capacity increased by approximately 64% with the application of geocell. In the numerical analysis, more displacement was observed at the bottom of the geocell wall than at the top. The position and type of load applied also affected the pressure distribution mechanism.

Biabani et al. (2016a) carried out experimental and numerical analysis of sub ballast reinforced with geocells. The loading applied was cyclic. ABAQUS was used to model the 3-D confinement provided by the cells to the soil. Sine function wave was used for load application to replicate the condition of the railway track. Experimental results were obtained by conducting tests on large-scale prismoidal triaxial apparatus. The axial and lateral deformation of the sub ballast decreased substantially after the application of geocells. More the stiffness of the geocell, lesser was the lateral deformation and more were the number of load cycles greater was the confining pressure. It was observed that with the increase in overburden pressure, the passive resistance increased with mobilization of tensile strength. Also, the confinement by cellular geocells leads to compression of the infill material. (Biabani et al., 2016)

Dash and Bora (2013) studied the provision of geocell and stone columns in weak soil. The results showed the bearing capacity of the soil increased by 3.6 when reinforced with a stone column and by 7.7 times when reinforced with geocell mattress. In the composite reinforcement- stone column and geocell, the bearing capacity enhanced by 10.1 times to the unreinforced soil. Apart from the increase in bearing capacity, a significant reduction in settlement of foundation soil was recorded. The effect of size and spacing of the stone columns in the presence of geocell reinforcement was also studied. The height of the geocell when increased more than the diameter of the footing showed a reduction in strength. This was due to the yielding and buckling of the geocell walls due to concentrated stresses on geocell boundaries which prevents mobilization of strength and stiffness due to geocell. The optimum height of the geocell and size of the stone column can increase the performance of the soil substantially.

Kumawat and Tiwari, (2017) conducted laboratory tests to study the effect of the geocell layer on the fly ash beds. The tests were conducted in a steel tank under the effect of square footing. The results were obtained by varying the dimensions and material properties of geocell. Strain in the geocell walls was recorded until failure occurred. The bearing capacity of the geocell reinforced fly ash beds increased by about 3.5 times than the unreinforced fly ash beds.

A study was conducted in the lab for determining the performance of geosynthetics-randomly distributed mesh, planar and geocell reinforcement in sand beds (Dash et al., 2004). Strip loading was applied in every test. Geocell reinforcement was found to be most beneficial among the three types of reinforcements. Compared with unreinforced soil, geocell reinforced soil took load eight times the ultimate bearing capacity of the soil and even at a settlement of 44% of the footing width, failure did not occur. While, in the case of planar reinforcement, failure was recorded when the settlement value reached 15% of footing width. In randomly distributed reinforced mesh case, at 1.7 times the ultimate bearing capacity of soil and settlement of 10% of the footing width, failure was recorded.

Lal et al. (2017) studied the effect of geocell and planar reinforcement, consisting of coir geotextile. The coir geotextiles are economical and have decent engineering properties, therefore, is suitable for developing countries. Plate load tests were conducted and square loading was applied. The geocell and planar reinforcement were made with the same amount of coir geotextile. The coir geocell enhanced the bearing capacity by 7.91 folds compared to 5.82 in the case of coir planar forms.

A. Hegde and Sitharam (2015) modeled the geocells in 3D finite-difference program to have a realistic approach in studying the performance of geocell. In comparison to geogrid reinforced and unreinforced soil, the geocell reinforced soil distributed load to a shallower depth. The load was distributed to a wider area in the lateral direction and reduced the vertical stress on the subgrade. Textured surface geocells showed better performance than with smooth-surfaced geocells. The strength of the foundation soil is influenced by the tensile strength and stiffness of the geocell. It was observed that the application of geogrid at the bottom of the geocell improved the performance of the soil by enabling the membrane mechanism.

A series of tests were carried out in the laboratory to understand the performance and load transfer mechanism of geocell reinforced sand beds. The deformation in the walls of geocells, subgrade deformation and load transmission and pressure distribution were observed during the experiments to study the geocell reinforcement mechanism (Dash, 2012). Geocell parameters, such as- geometry and material of the geocell and depth of placement of geocell mattress were kept variable. The strain variation pattern of the geocell walls indicated that the geocell mattress behaves as a composite beam supported by the subgrade soil. To make the geocells, geogrids of different types were used. Strength and stiffness studies were carried out by varying the aperture opening size and orientation of the rib of the geocell material. Geocells made of higher strength geogrids and with less aperture opening size showed better performance.

The behaviour of strip footing on the sandy layer was studied by carrying out finite-element simulations (Latha et al., 2009). The effect of the height of the geocell and infill material in geocell on the strength and stiffness of the sand layer was analyzed. By performing triaxial tests on geocell reinforced soil, a composite model with similar characteristics was obtained in terms of empirical equations. The results of the experiments-load settlement curve, matched with the numerical simulation result. The shear contours were observed to be shifted downwards and enlarged horizontally, indicating the transfer of load to a larger area.

Hegde (2017) provided a summary of the past, present and future scope of geocell application. The study represented the evolvement of the geocell on ground improvement and provided a future scope of its application in foundations, pavements, railways, retaining walls and protection of the underground utilities.

Leshchinsky and Ling, (2013a) performed a series of laboratory tests to study the most appropriate configuration of the geocell to obtain the best results. The geocell mattress was reinforced in embankment and stiffness, strength and deformation behavior were compared. The confinement due to geocell reduced the settlement and horizontal spreading of the granular soil. In the case of cyclic loading, the continuous vertical settlement was observed. The stress and strain were found maximum at the bottom corners of the geocells, lying below the load. High tensile stress resulted in more vertical displacement below the loading plate. Enough seam strength should be there to prevent the geocell failure. Though it was pointed in the study that field testing would validate the results and also help in understanding the phenomenon like the effect of cyclic loading, creep and foundation to some extent. Leshchinsky and Ling, (2013b) studied the application of geocell in railway sub-ballast by finite element simulations. Ballast strength was varied to simulate the track material and foundation stiffness to replicate the subgrades. The effect of stiffness of the geocell was also analyzed. The geocell mattress was found to be more effective when the ballast material was weak. The vertical deformations reduced to some extent due to the confinement provided by the geocell to the ballast. The distribution of the stresses was more uniform in the case of softer subgrades resulting in a decrease in the shear deformation.

The study of embankment construction on soft soil was carried out in another study (Latha et al, 2006). The geocells were made by using geogrids. A setup was prepared in the laboratory. The load was applied in the form of a strip. The maximum load capacity without failure was obtained and strain values on the geocell surface were monitored. The study regarding the geometry of the geocell-height, internal diameter and material, and infill soil of geocell was made. The laboratory results were validated by the slope stability program. (Madhavi et al, 2007). The geocell application improved the bearing capacity and decreased settlement substantially.

In another study, different geosynthetics – geocell, planar reinforcement and randomly distributed mesh were used as reinforcement under a square footing in the sandy foundation (Madhavi Latha and Somwanshi, 2009). Biaxial geogrids and geonets were used to form the required geosynthetics. The quantity of the reinforcement for each case was kept the same. Through experiment and numerical analysis, it was found that the geocell reinforcement gave the best result among the three types of reinforcements. Geogrid formed by randomly distributed elements of mesh was found inferior to the other two forms.

Mamatha and Dinesh, (2017) carried out an analysis to check the ruts formation on pavements constructed on weak subgrades. The loading of 761 kPa was applied in the form of a haversine function to simulate vehicle loading. The test was done for 500 cycles of loading. The ruts formation was mainly due to the plastic-settlement of the subgrade. The application of geocells reduced the rutting up to 12-70% and therefore increased the life of the pavement by 1.5-3.4 times with varying thickness of the pavement and aspect ratio. The heaving on the soil also reduced marginally. Moreover, the provision of geocell in the subgrade and sub-base results in better durability with no environmental impacts.

Another study was done in PLAXIS 2D to find the stability of embankment slopes by varying the height and side slope of the embankments (George and Marathe, 2016). The factor of safety for each case was determined. The test was carried out in the Kannad region, India on laterite soil. The soil was found to be stable and appropriate for embankment construction.

Sri and Tjandra, (2015) investigated the performance of the road embankment when reinforced with geotextile by varying the length of the geotextile. The safety factor was determined which mainly depended upon the tensile strength of the geotextile.

Mehdipour et al., (2013) studied the load transfer mechanism of slope reinforced with geocell. The geocell behavior was simulated by the beam model. The geocell mattress behaved like a flexible slab which transferred the bending and concentrated stresses on the geocell walls to the foundation soil. The study concluded that with geocell provision at the mid of the slope failure surface without reinforcement and slope surface reduced lateral and shear strain considerably.

Mehdipour et al., (2017) analytically determined the safety factor of slope reinforced with geocell. A horizontal slice method was used in the study. It was observed that the height of the geocell mattress significantly affects the performance of the geocell. The greater the height of the geocell more was the mobilization of frictional resistance and flexure strength. For achieving the same safety factor, a lesser quantity of geocell reinforcement was required in comparison with planar reinforcement.

Series of laboratory tests to understand the potential advantages of reinforcement of geocells over the clayey layer with a void were carried out (Sireesh et al., 2009). Effect of size of geocells, the relative density of the soil in geocell pockets, the effect of applying planar geogrid at the base of the geocell layer was studied. The void did not show any effect in bearing capacity when the geocell spread by twice the size of the void on both sides of the void. When the thickness of the geocell layer was greater than 1.7 times the width of the footing, the influence of the void was not much. More the denseness of the infill soil of geocell opening more was the improvement in strength.

A study was conducted to know the effect of geocell reinforced in expansive strata (Kumar et al. 2019). Polypropylene geotextiles were used to make chevron type geocells. It was concluded that by using geocells of optimum dimensions and at the appropriate depth, the load-bearing capacity of the soil increased by 210% and settlement reduced by 80%.

Tafreshi et al., (2014) conducted tests to study the behavior of geocells reinforced with granulated rubber over weak foundation soil. The loading was cyclic. The use of granulated rubber decreased the plastic settlement by 65 % and increased resilient deformation compared to the unreinforced case. It also resulted in even distribution of stress to the foundation bed.

On a soft soil foundation, geosynthetics were placed to study the improvement in the performance of the soil (Zhou and Wen, 2008). Sandy soil was used as infill for geocell openings. For geocell reinforced soil, the coefficient of subgrade reaction increased by 300% and settlement decreased by 42% of the unreinforced soil. Less heaving on the earth's surface was observed in the presence of geocell reinforced sandy soil overlaying on soft soil bed.

CHAPTER 3

NUMERICAL MODELLING

A total of 8 tests have been performed in PLAXIS 2D Version 8. In the first case, a model without geocell reinforcement has been prepared for comparison with the performance of geocell reinforced embankment.

3.1. MATERIALS

The properties of foundation soil and embankment soil used in the study are listed in Table.3.1 and Table.3.2.

Table.3.1. Properties of foundation soil

PROPERTY	VALUE
Cohesion	10 kPa
Unit weight	17 kN/m^3

Table.3.2. Properties of embankment soil

PROPERTY	VALUE
Cohesion	10 kPa
Internal angle of friction	30 kPa
Unit weight	19 kN/m^3

The properties of the geocell used in the study is given in table.3.3. The geocell openings are triangular in shape and the pocket size of geocells is 0.4m for all cases. The equivalent diameter (d_e) has been obtained by equating the triangular area of geocell opening with the area of the circle. The diameter of the circle is the equivalent diameter of cells. This gives the value of the equivalent diameter of the geocells as 0.2256m.

Three types of geocells have been used in the study. The height of BG geocell mattress (h) has been varied- 100mm, 150mm and 200 mm to understand the effect of the height of geocell on load-bearing capacity of the soil. A comparison of the effect of infill material of geocell pockets-clay and sand has also been done.

Table 3.3 Properties of geocell (Madhavi Latha et al. 2006)

Type of geogrid used for making geocells	Height of geocell layer h(m)	Secant modulus of geogrid M (KN/m)	Additional confining stress due to geocells $\Delta\sigma_3$ (kPa)	Additional cohesion due to geocell layer C_r (kPa)	Cohesive strength of geocell layer C_g (kPa)	Φ of geocell layer (degrees)
Unreinforced	-	-	-	-	-	-
UG	0.10	200	47.8	41	51	30
BG01	0.10	160	37.1	32	42	30
BG015	0.15	160	37.1	32	42	30
BG02	0.20	160	37.1	32	42	30
BG01 (clay)	0.10	160	25.5	13	23	0
NG-1	0.10	70	16.4	14	24	30
NG-2	0.10	70	22.5	19	29	30

3.2 COMPOSITE MODEL OF GEOCELL ENCASED SOIL

Bathurst and Karpurapu (1993) and Rajagopal et al., (1999) conducted tests on geocell reinforced sand and found out that an apparent cohesion is induced due to confinement by geocells. The angle of internal friction remained the same as that of the infill soil. This was concluded by results of direct shear tests on geocell encased soil.

The value of induced cohesion(C_g) is given by the equation:

$$C_g = \frac{\Delta\sigma_3}{2}\sqrt{K_p} \qquad (1)$$

In eq. $\Delta\sigma_3$ is increase in the confinement due to the geocell and K_p is the coefficient of passive earth pressure. Henkel and Gilbert (1952) suggested that the behaviour of soil encased in geocells is similar to a thin cylinder subjected to internal pressure and gave the following equation based on the theory of hoop tension:

$$\Delta \sigma_3 = \frac{2M}{d_0} \frac{1-\sqrt{1-\varepsilon_a}}{1-\varepsilon_a} = \frac{2M\,\varepsilon_c}{d_e} \frac{1-\sqrt{1-\varepsilon_a}}{1-\varepsilon_a} \tag{2}$$

Where ε_a=axial strain at failure

d_0=initial diameter of the individual cell

d_e = equivalent diameter of the cell

M = modulus of the geocell material corresponding at an axial strain of ε_a (calculated by the load-strain test) (kN/m)

$$\varepsilon_c = \frac{1-\sqrt{1-\varepsilon_a}}{1-\varepsilon_a} \tag{3}$$

Madhavi and Rajagopal (2001) gave the value of modulus of geocell reinforced soil by correlating the elastic modulus of infill soil and secant modulus of geocell material. The empirical equation was obtained by conducting triaxial compression tests on geocell encased soil. The equivalent modulus of geocell encased soil (E_g) is given by:

$$E_g = E_s + 200M^{0.16} \tag{4}$$

Where E_s is a dimensionless modulus parameter of unreinforced soil which is a modulus number in the hyperbolic model given by Duncan and Chang (1970).

3.3 GEOMETRY OF THE MODEL

Madhavi Latha et al (2006) conducted laboratory tests to study the performance of geocell reinforced embankment. Fig.3.1 shows the laboratory setup of the model used for the study. The same model has been made in the PLAXIS software.

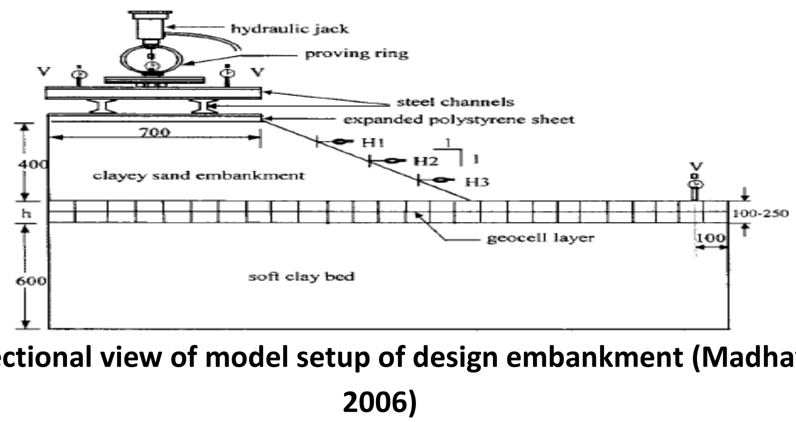

Fig.3.1. Sectional view of model setup of design embankment (Madhavi et al. 2006)

3.4. FEM MESHING AND BOUNDARY CONDITIONS

A laboratory model of the embankment is 1000 mm high and 1800 mm long having a slope gradient of 1:1. The embankment was constructed in two 200 mm thick layers. The foundation layer consists of clayey soil of 600mm. The embankment top width is 700mm. The embankment was assumed symmetric and therefore only half of the embankment is considered in the finite-element analyses. The plane strain condition and fifteen- node triangular elements were used.

3.5. MATERIALS

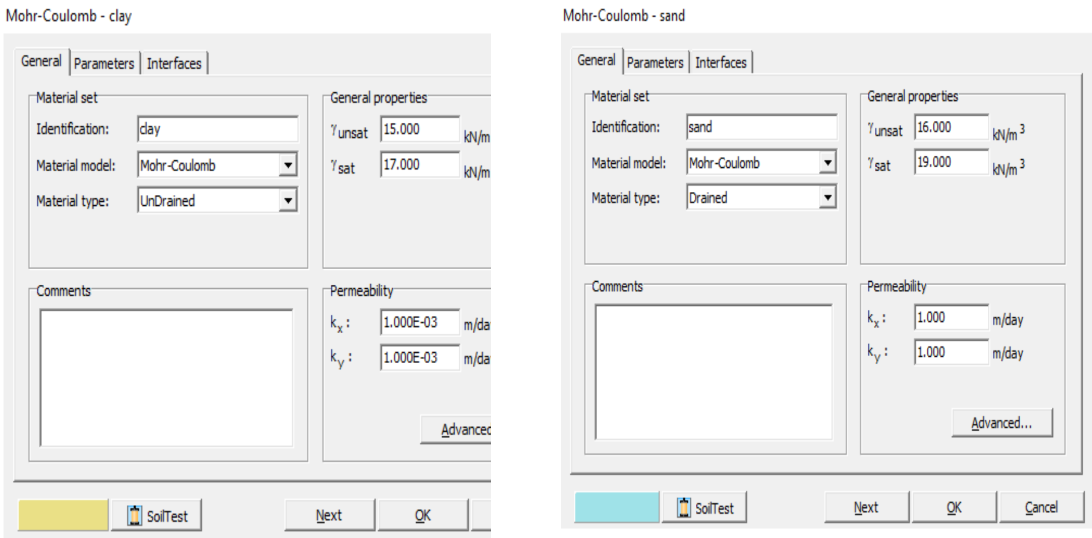

(a)

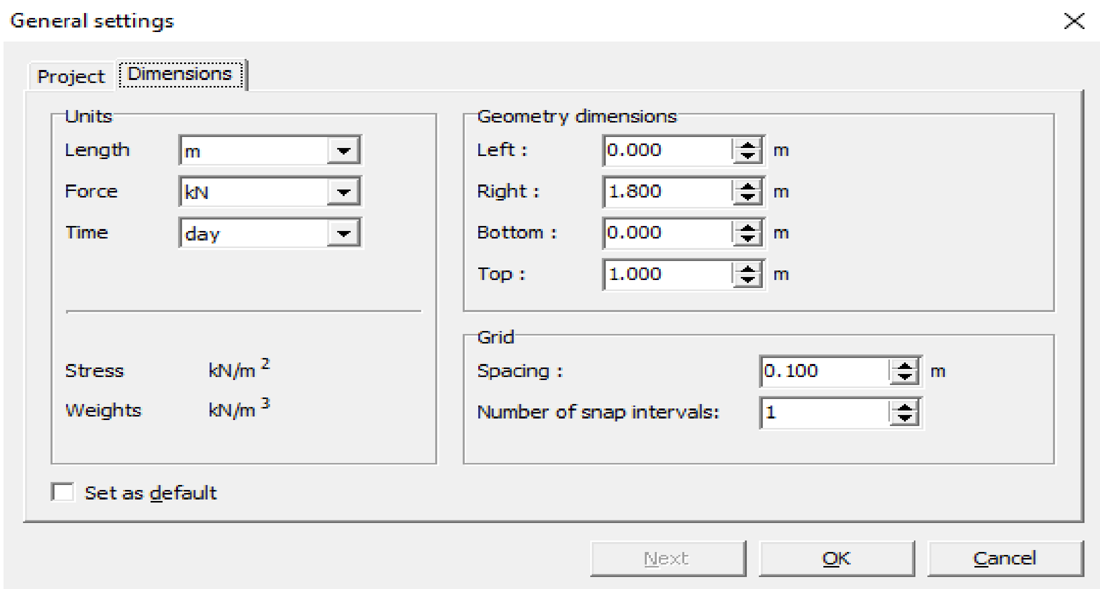

(b)

Fig.3.2. Input-soil properties and dimensions of the model (Unreinforced)

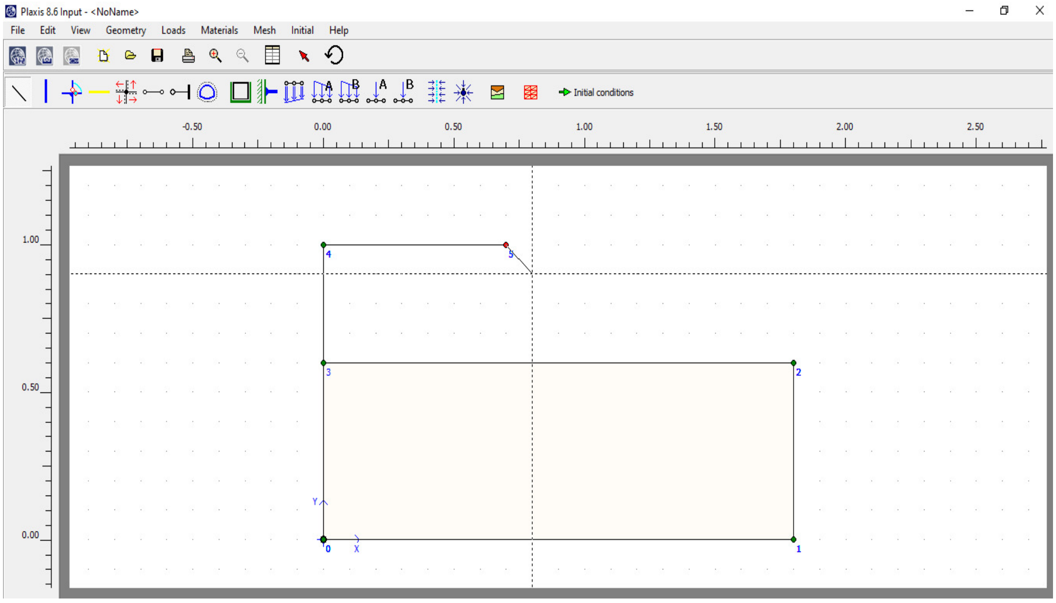

Fig.3.3. Geometrical construction of the model (unreinforced)

The upper boundary formed by the embankment and the existing ground surface is left free to displace. Jaky's formula ($K_0 = 1 - sin\emptyset$) is used to calculate the coefficient of lateral earth pressure.

Input the foundation and embankment soil characteristics, assign the properties to the soil layers and define the geometry of the model as shown in Fig. 3.2. (a) and (b).

3.6 BOUNDARY CONDITIONS

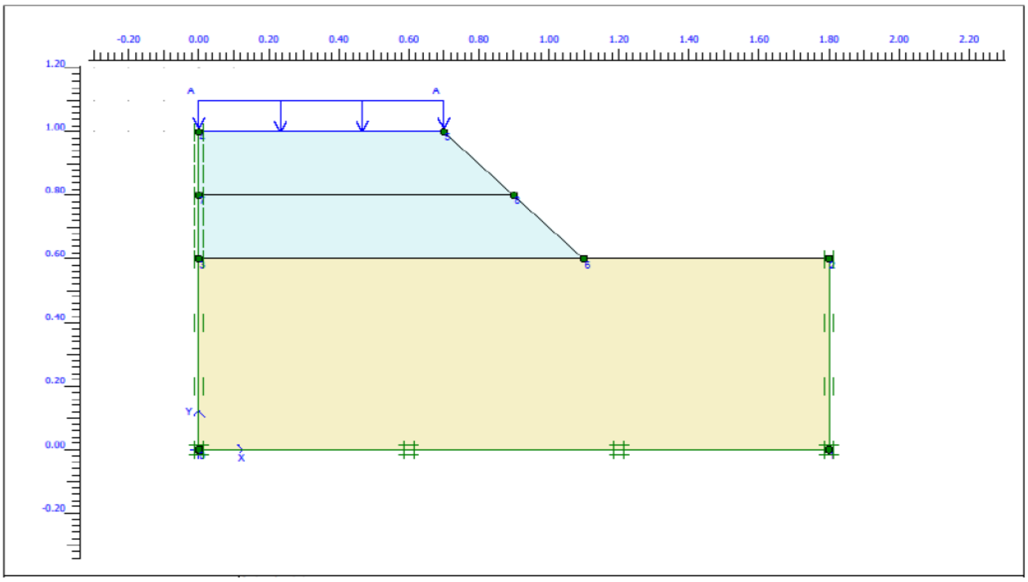

Fig.3.4. Geometry of the model after application of surcharge load (Unreinforced)

The displacement boundary conditions, on the y=0 axis, were defined as taking horizontal displacement (U_x) and vertical displacement (U_y) as 0, simulating the boundary of the steel tank as hard strata. The nodes of the vertical boundaries, x=0 and x=1800mm, were fixed against horizontal movement but allowed to move freely in the vertical direction.

Generate the mesh by choosing the mesh coarseness (Fig.3.5).

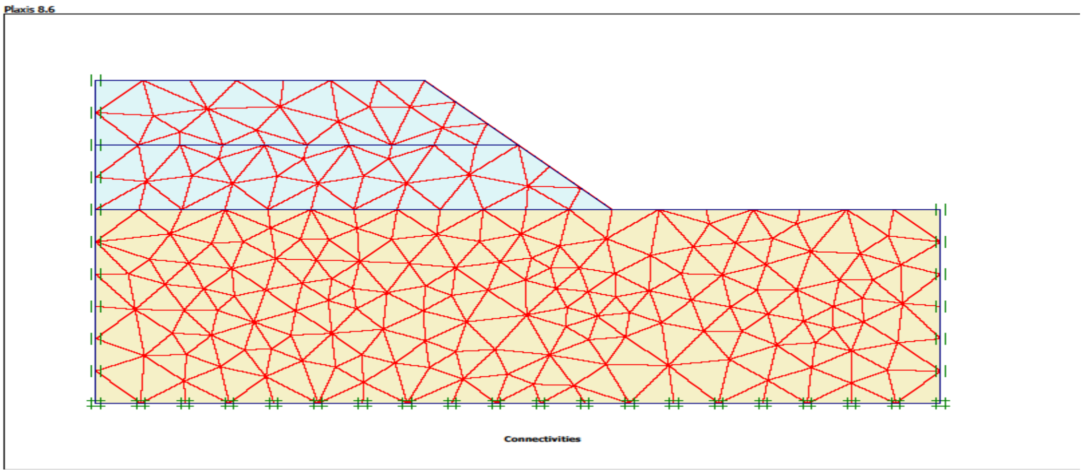

Fig.3.5. Generated mesh (Unreinforced)

Assign the water level and generate pore water pressure. In this case, there is no water table. (Fig.3.6)

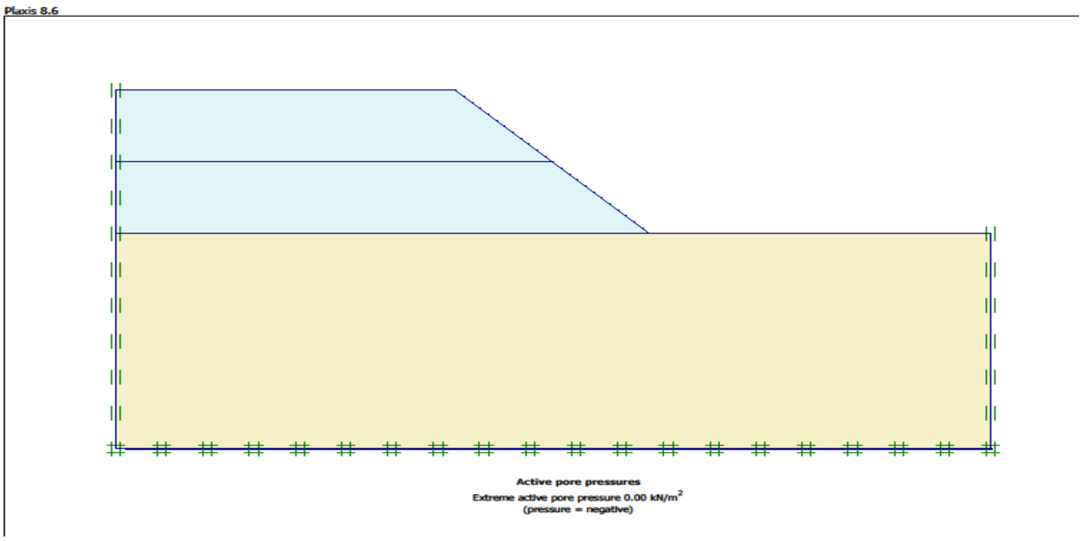

Fig.3.6. Active pore water pressure (Unreinforced)

Select the model geometry while generating the initial stresses. The stresses are generated before the embankment construction (Fig.3.7).

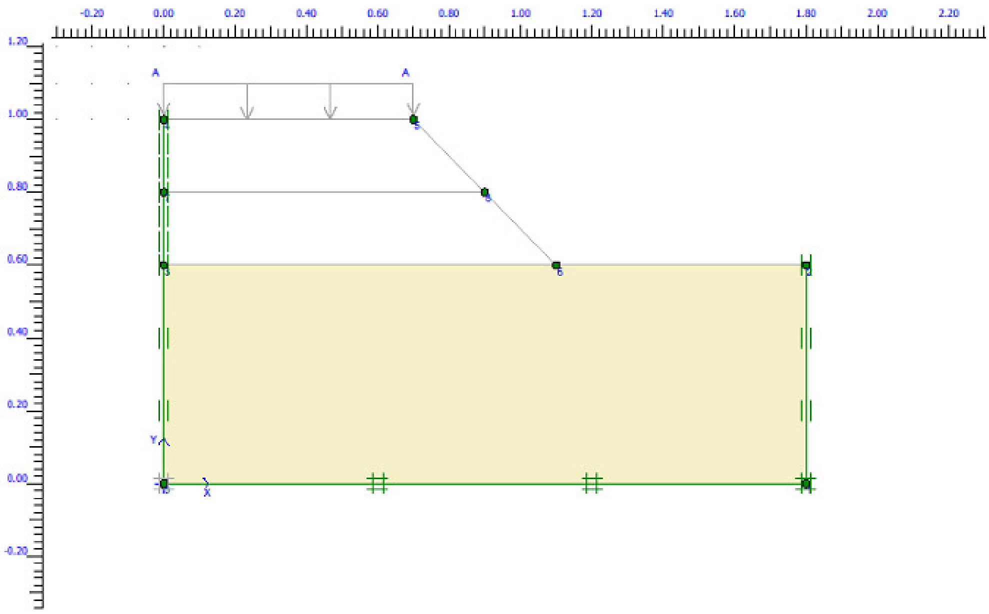

(a)

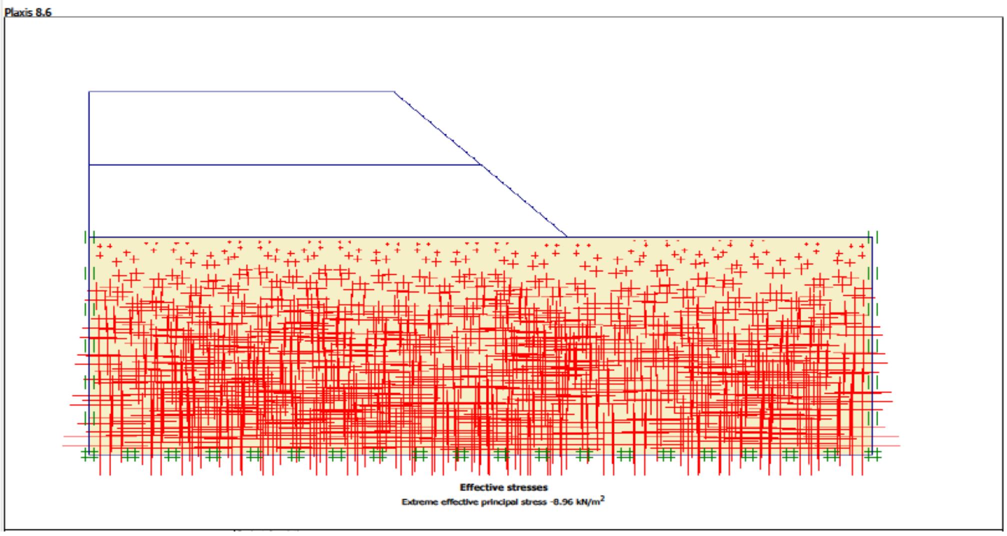

(b)

Fig.3.7. Initial stress generation (Unreinforced)

The calculation phase is divided into three stages for the construction and application of load on the embankment. All the three stages have been modelled as plastic staged construction. All stages are modelled as Consolidation – Staged Construction phases. The three stages are:

i. The construction of a 200mm embankment above the foundation soil.

ii. The construction of 200mm embankment followed by step 1, which make the total height of embankment 400mm

iii. Application of surcharge

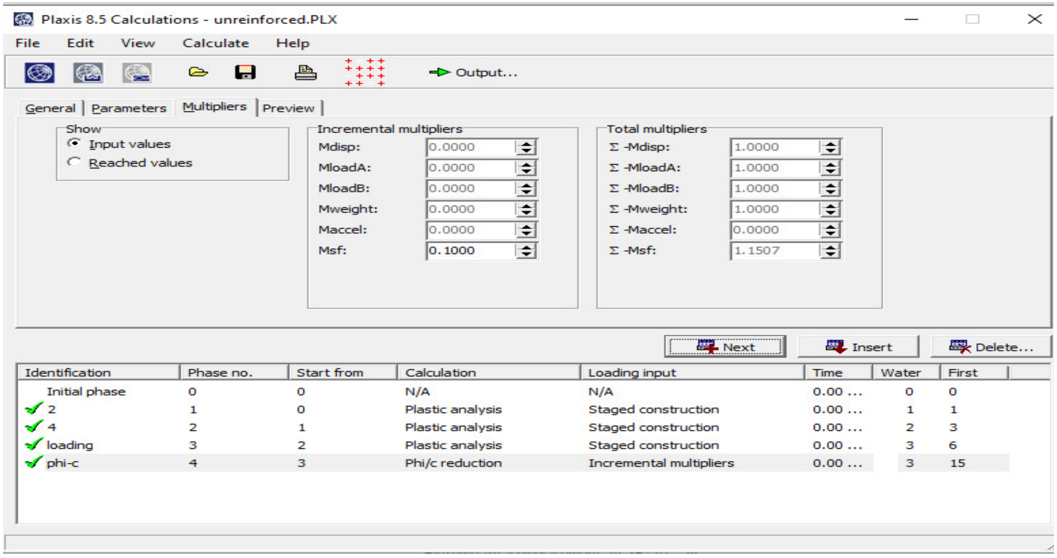

Fig.3.8. Calculation stage (Unreinforced)

The phi-c reduction is an additional step done to obtain the Msf value. Msf is the factor of safety of slope.

The same steps, as in the case of the unreinforced embankment, are followed for all the other cases of geocells-UG, BG and NG. The only additional step is the application of the geocell mattress at the base of the embankment. The geocell layer is transformed into an equivalent soil layer by the empirical equations given in section 3.2 of the report.

The steps for constructing embankment reinforced with geocell (UG01) have been given in detail below. Similar steps have been followed for other types of geocell reinforcement.

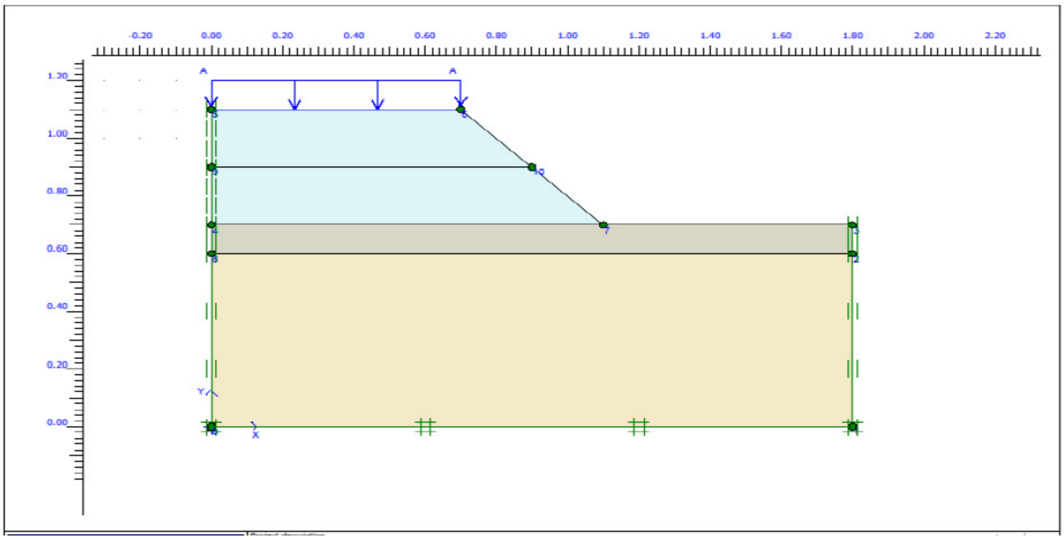

(a) Geometry of the model (UG01)

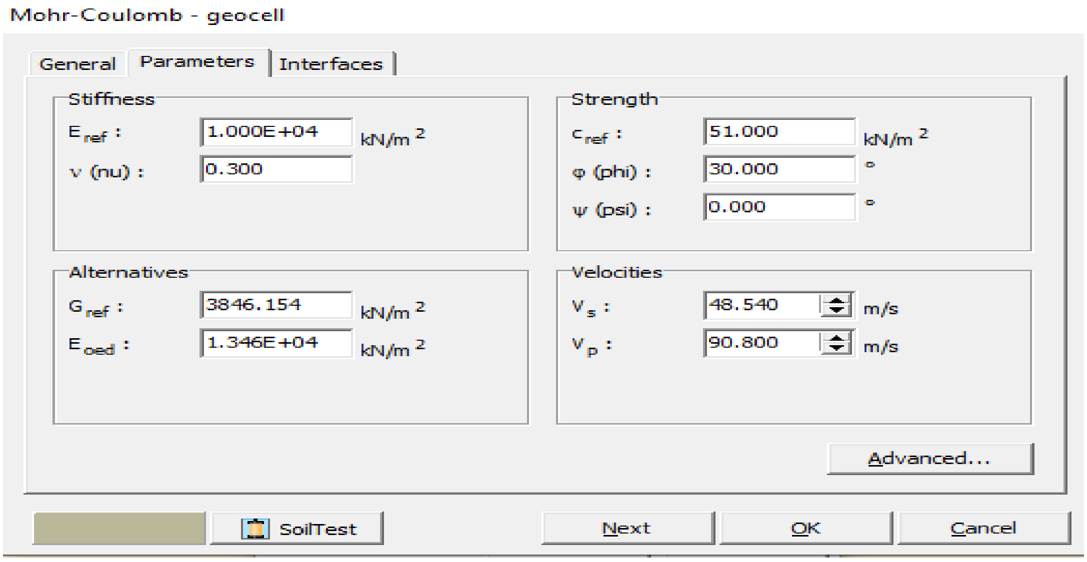

(b) Assigning geocell reinforced layer as an equivalent soil layer, from table 1 (UG01)

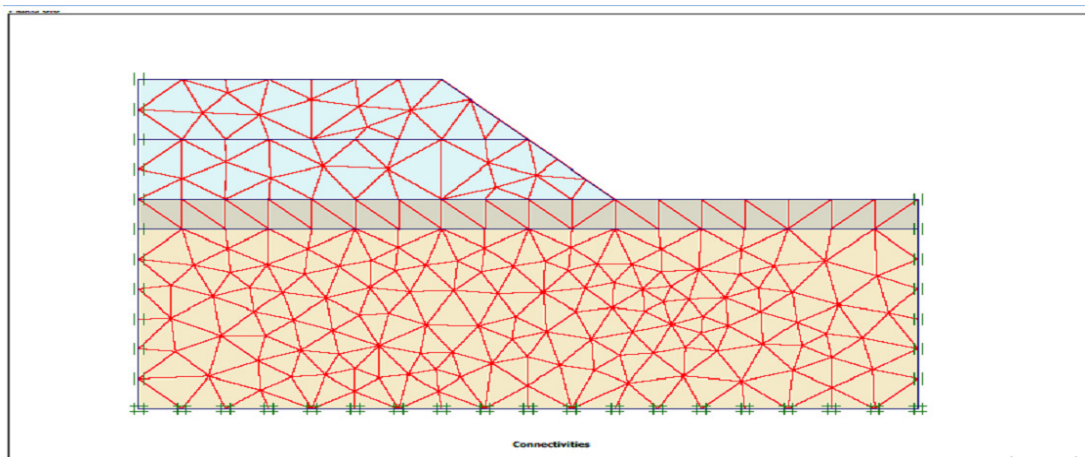

(c) Generated mesh (UG01)

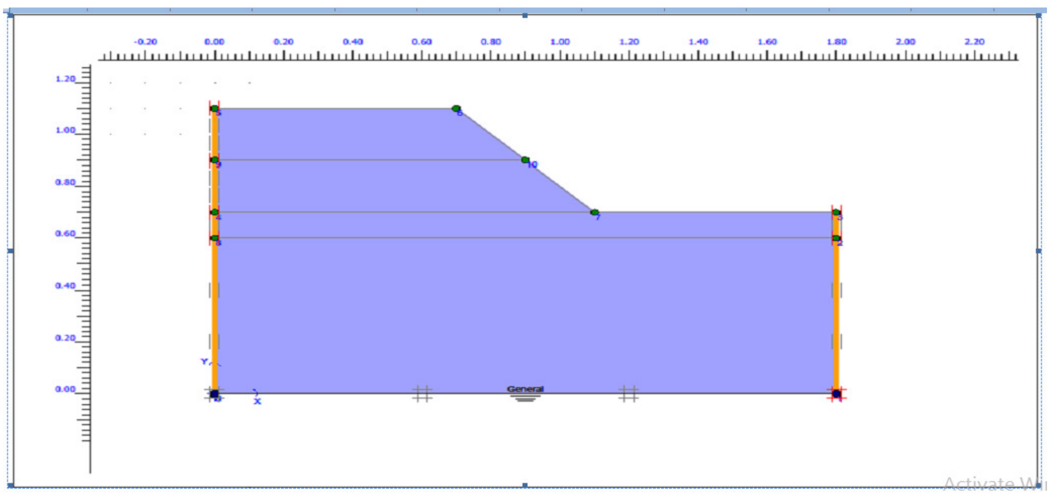

(d) No pore water pressure (UG01)

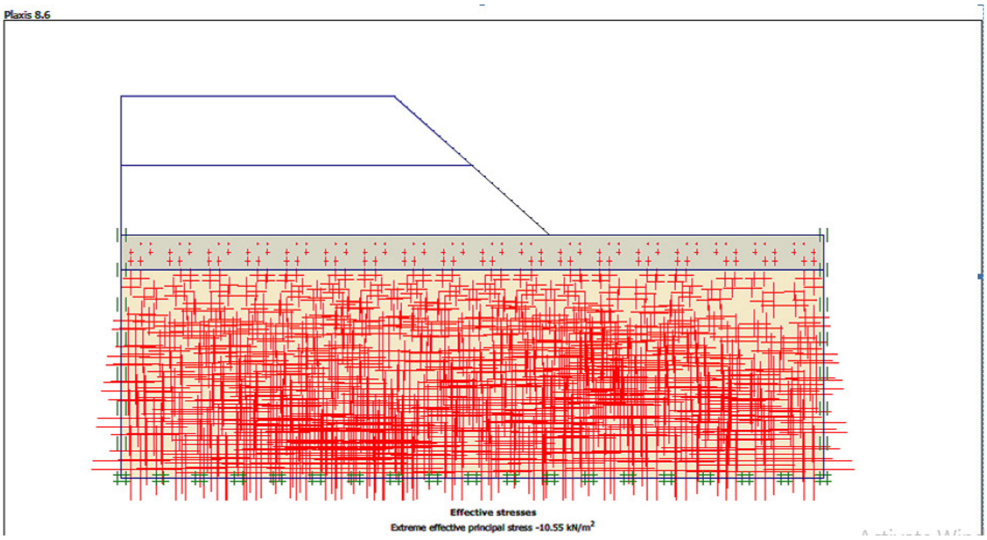

(e) Initial effective stress generated (UG01)

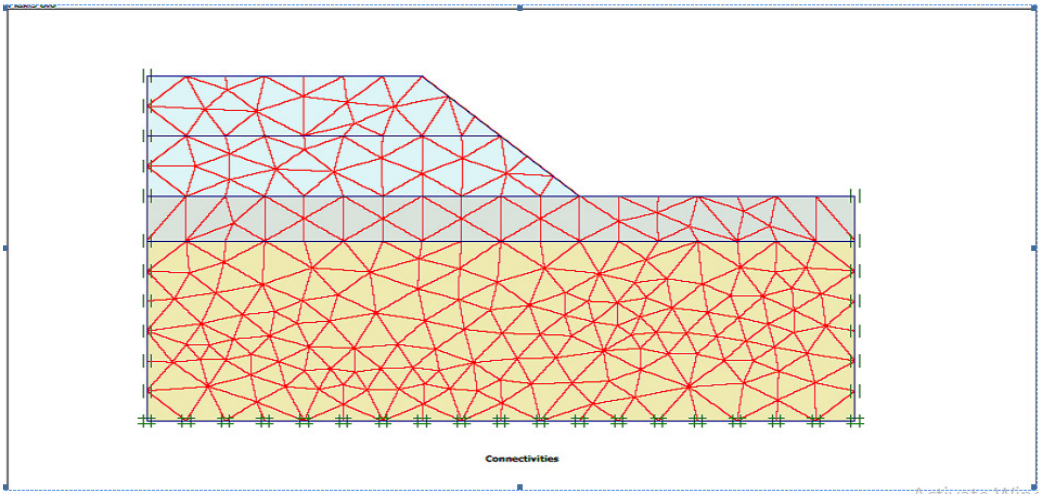

(f) Generated mesh (UG01)

Fig. 3.9. Steps for construction of geocell (UG01) reinforced embankment

The mesh as shown above has been generated in a similar way for all embankment reinforced with other types of geocell.

CHAPTER 4

RESULTS AND DISCUSSION

The deformed mesh and factor of safety achieved in each case, unreinforced and geocell reinforced embankment, have been presented as the output.

UNREINFORCED EMBANKMENT

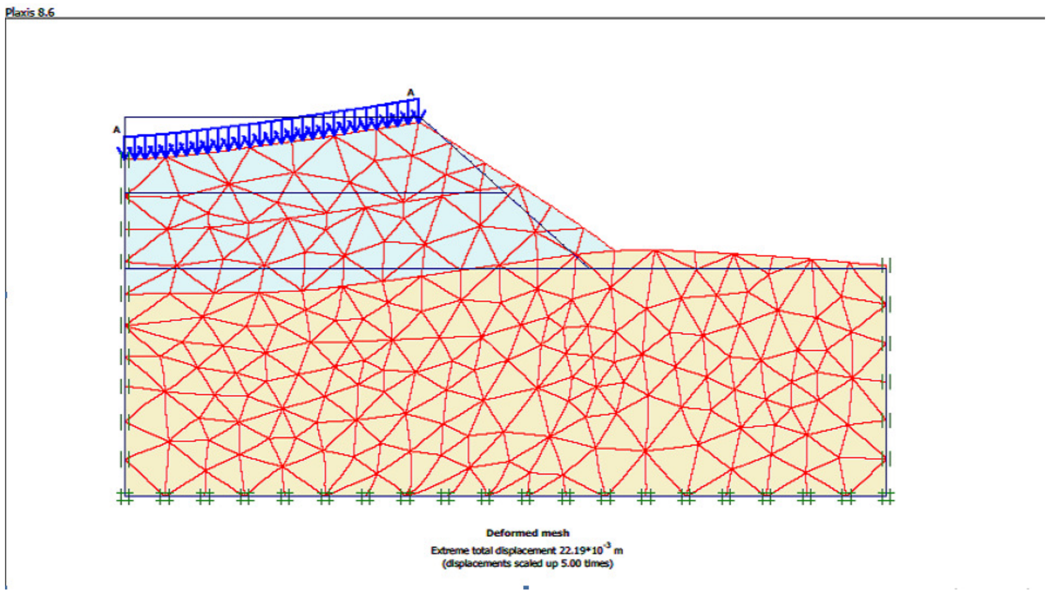

(a) Deformed mesh

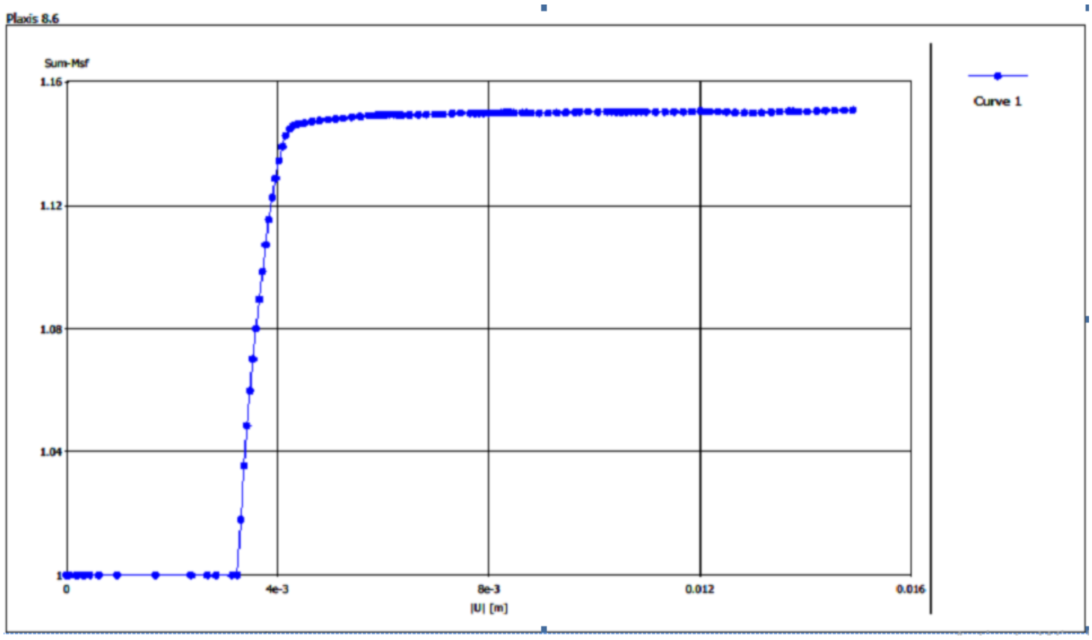

(b) Factor of safety

Fig.4.1. Deformed mesh and FOS for unreinforced embankment

UG01 GEOCELL-

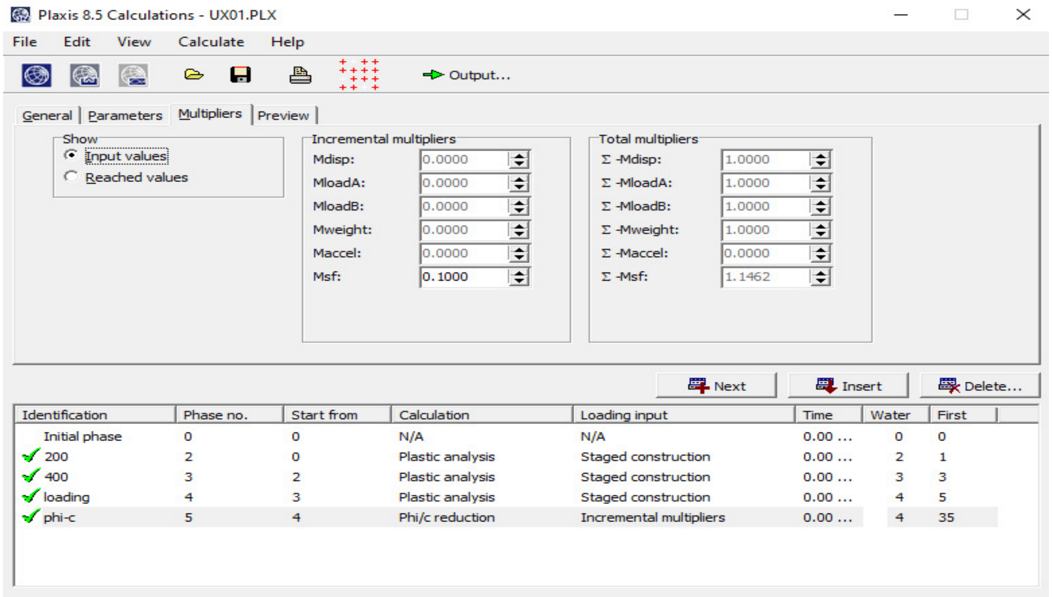

(a) Calculation phase

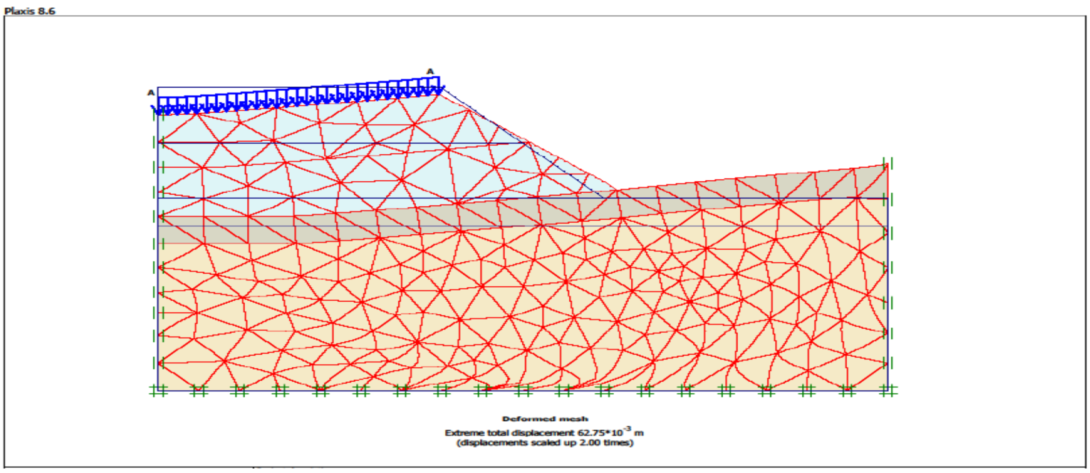

(b) Deformed mesh

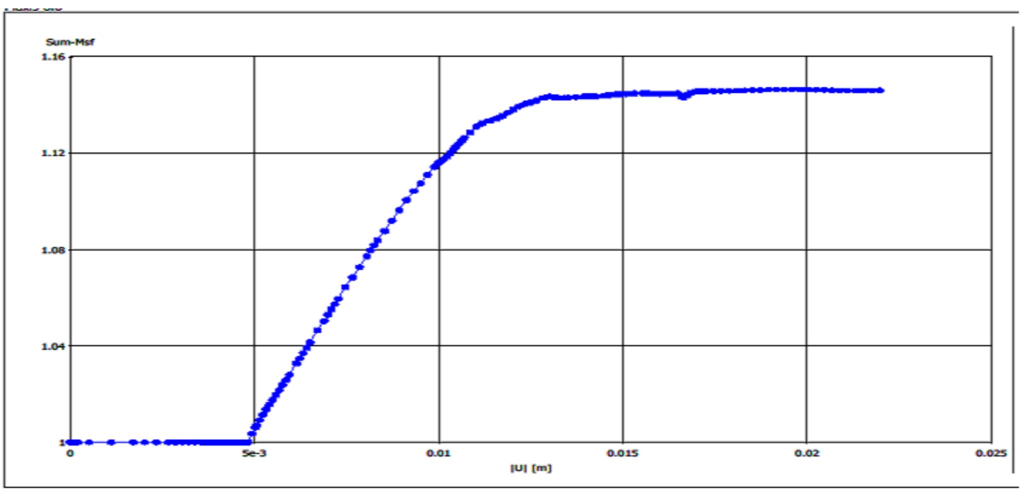

(c)Factor of safety (UG01)

Fig.4.2.Calculation stage, deformed mesh and FOS for UG01 geocell reinforced embankment

BG01 GEOCELL-

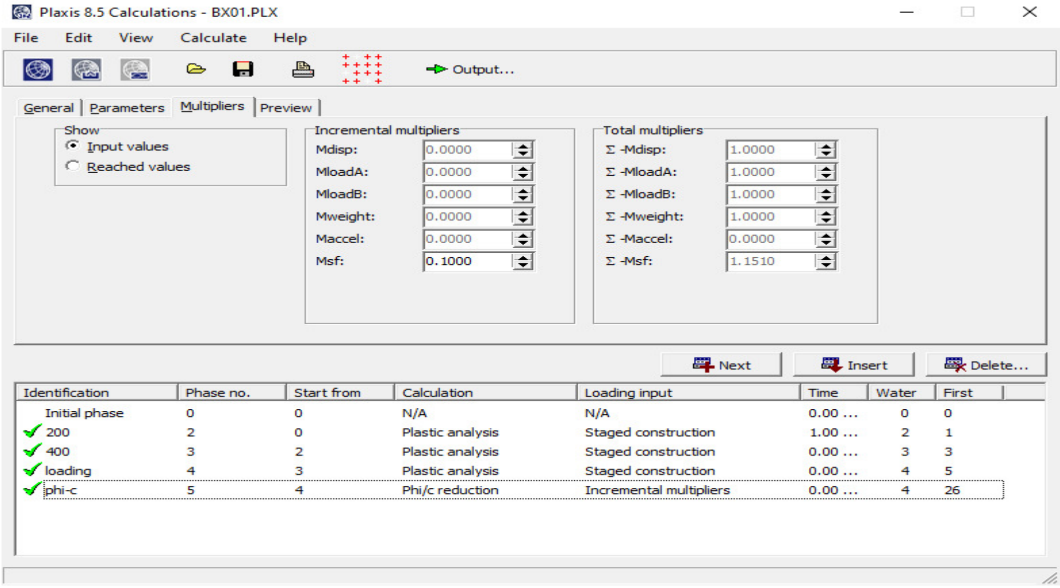

(a) Calculation phase

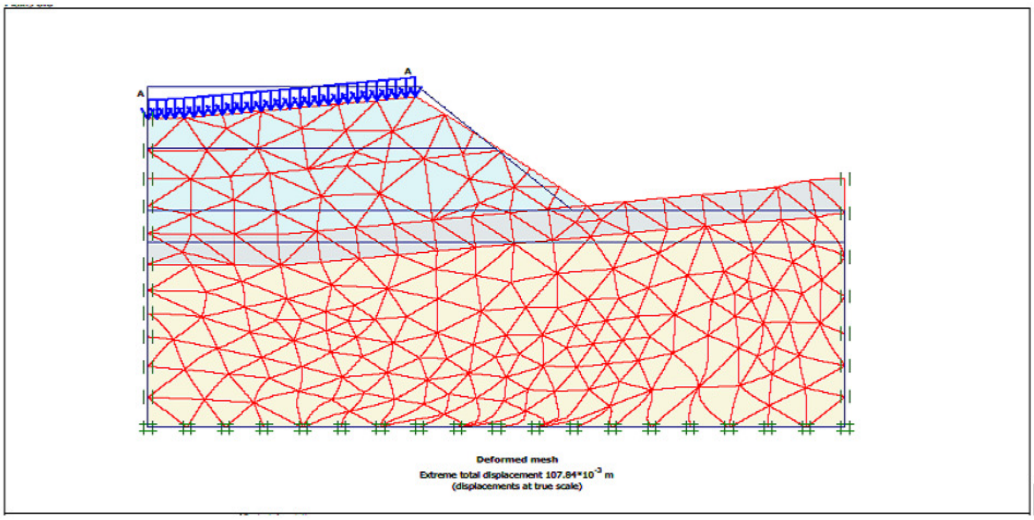

(b) Deformed mesh

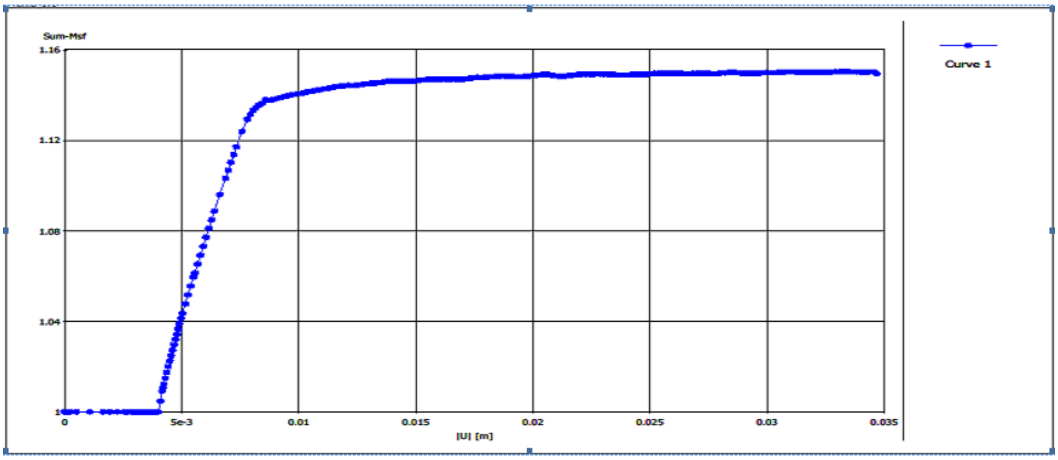

(c) Factor of safety

Fig.4.3.Calculation stage, deformed mesh and FOS for BG01 geocell reinforced embankment

BG015 GEOCELL-

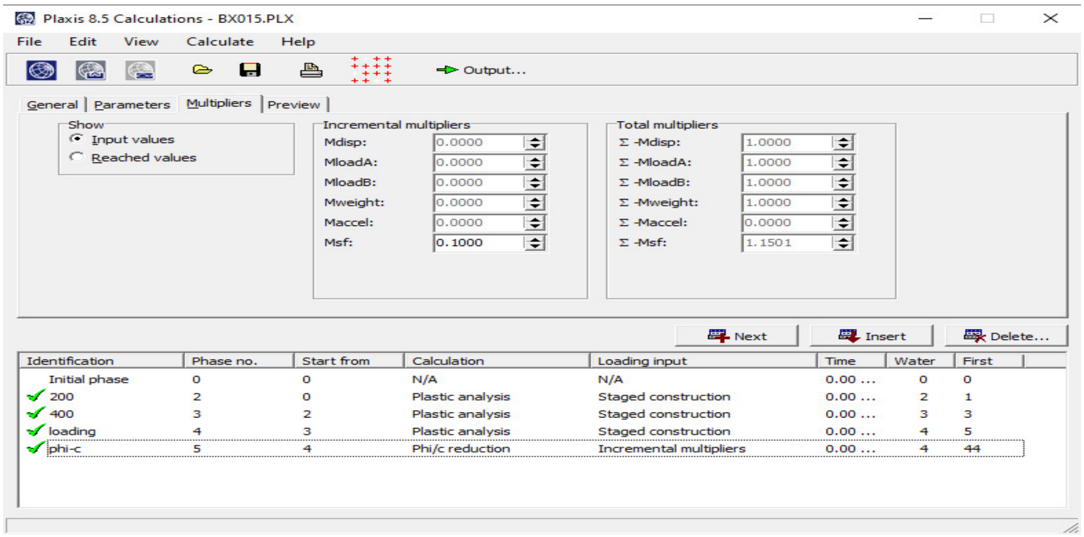

(a) Calculation phase

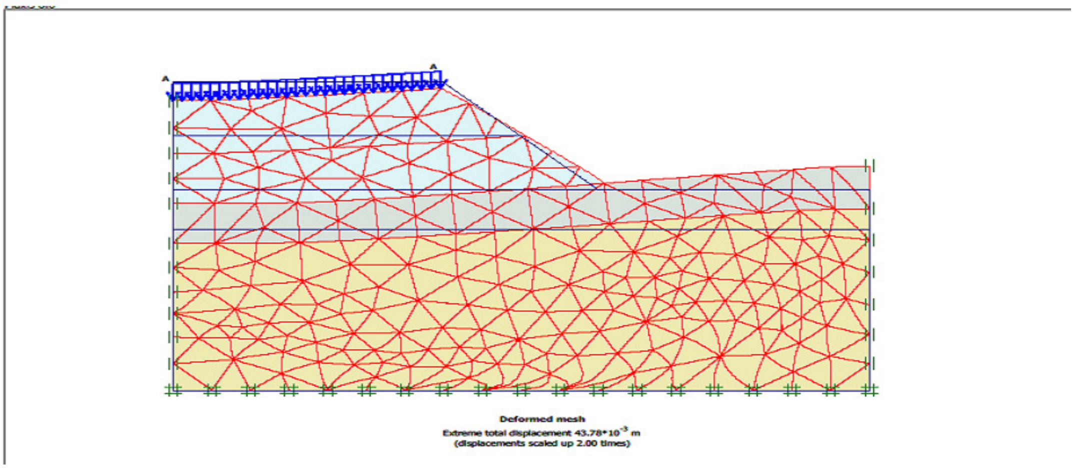

(b) Deformed mesh

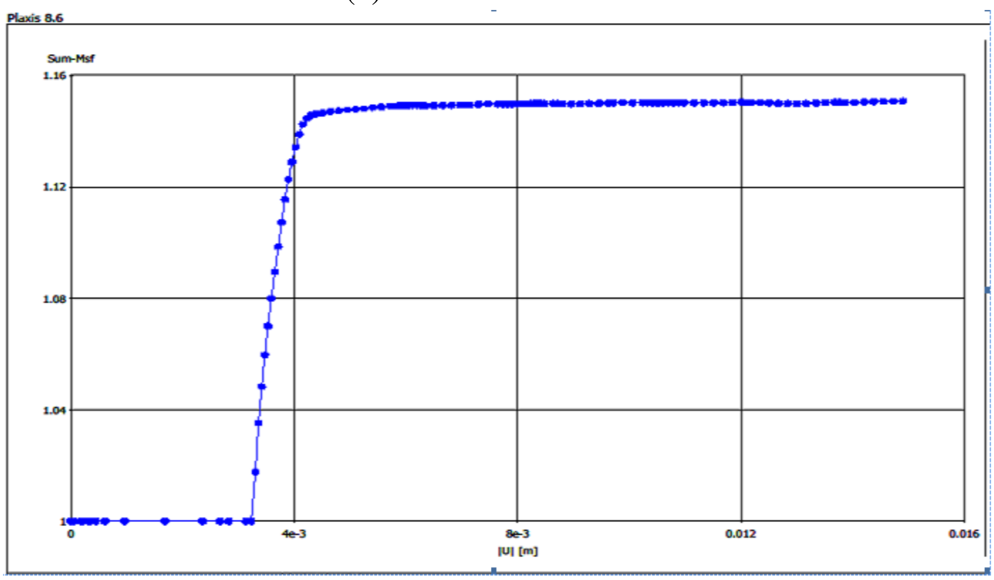

(c) Factor of safety

Fig.4.4.Calculation stage, deformed mesh and FOS for BG015 geocell reinforced embankment

BG02 GEOCELL-

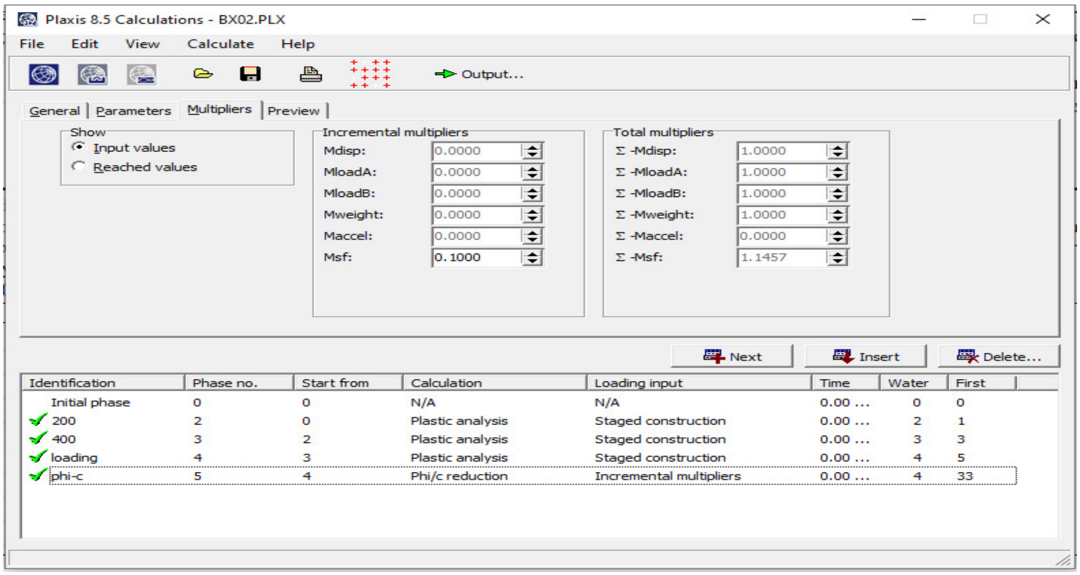

(a) Calculation phase

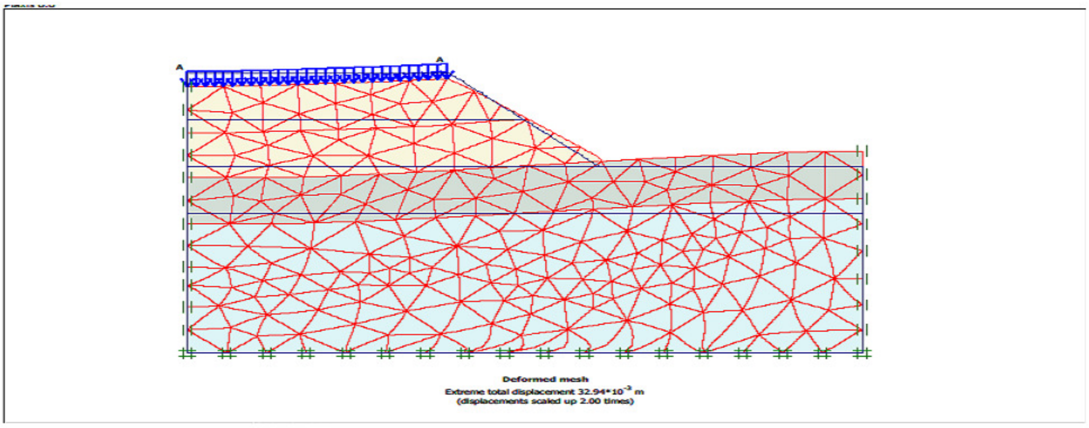

(c) Deformed mesh

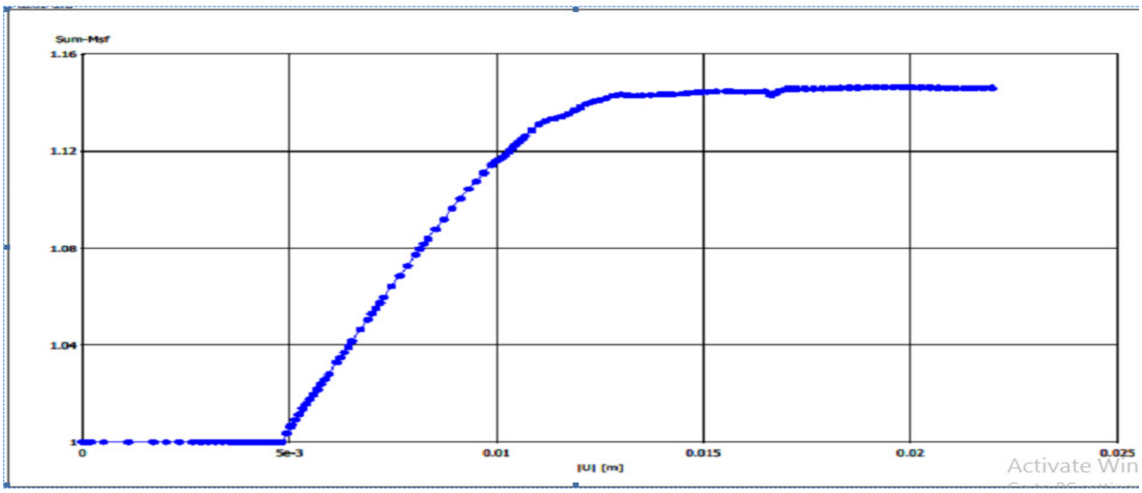

(c) Factor of safety

Fig.4.5.Calculation stage, deformed mesh and FOS for BG02 geocell reinforced embankment

BG01(CLAY)-

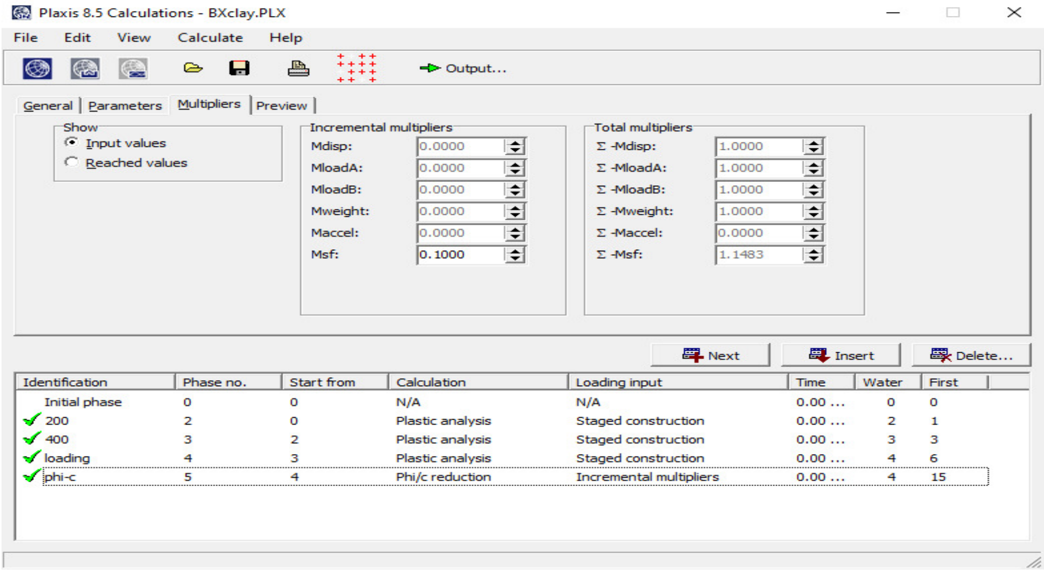

(a) Calculation phase

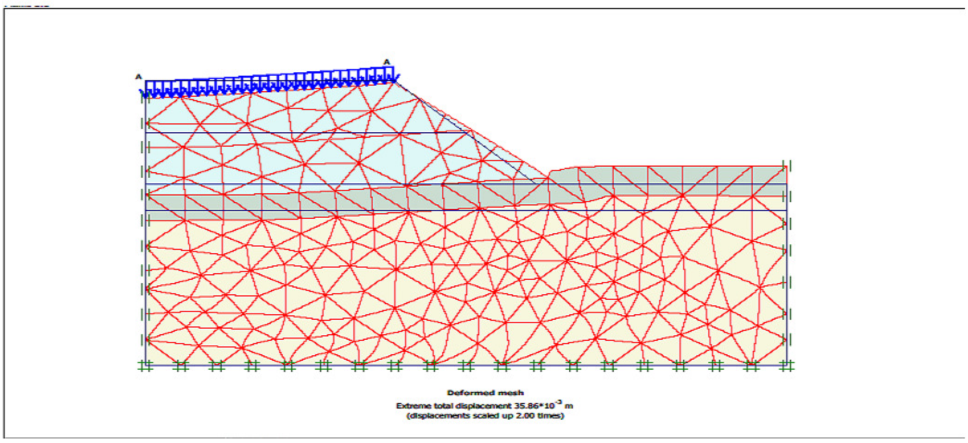

(b) Deformed mesh

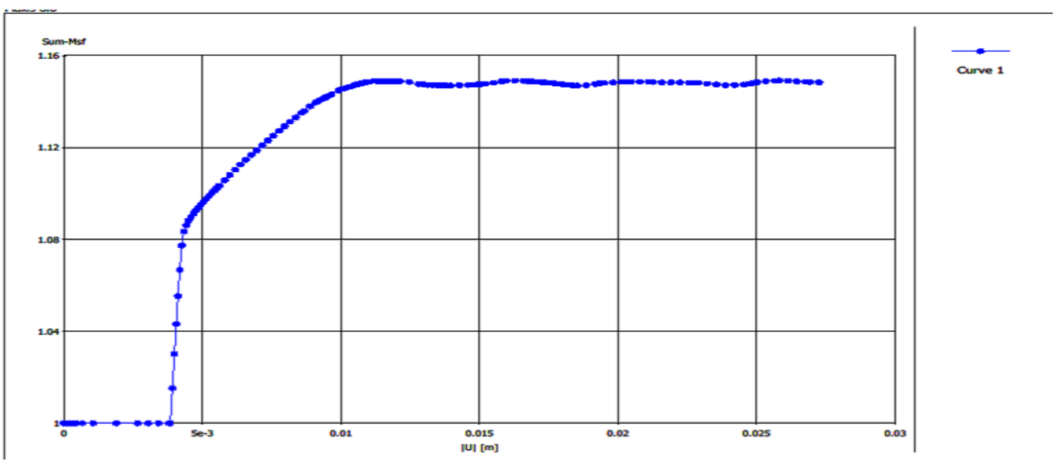

(c) Factor of safety

Fig.4.6.Calculation stage, deformed mesh and FOS for BG01(clay) geocell reinforced embankment

NG1 GOECELL-

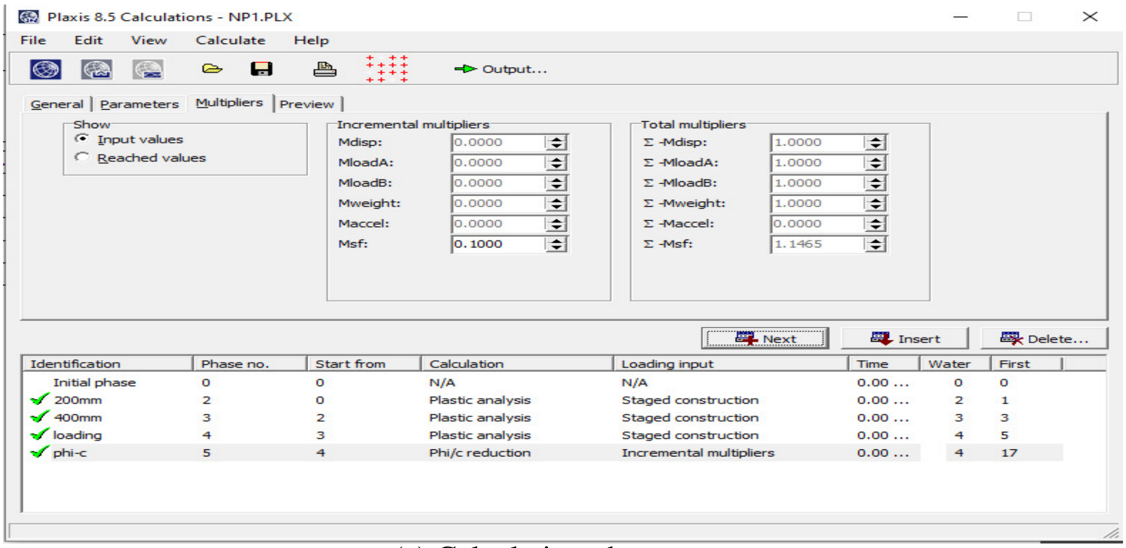

(a) Calculation phase

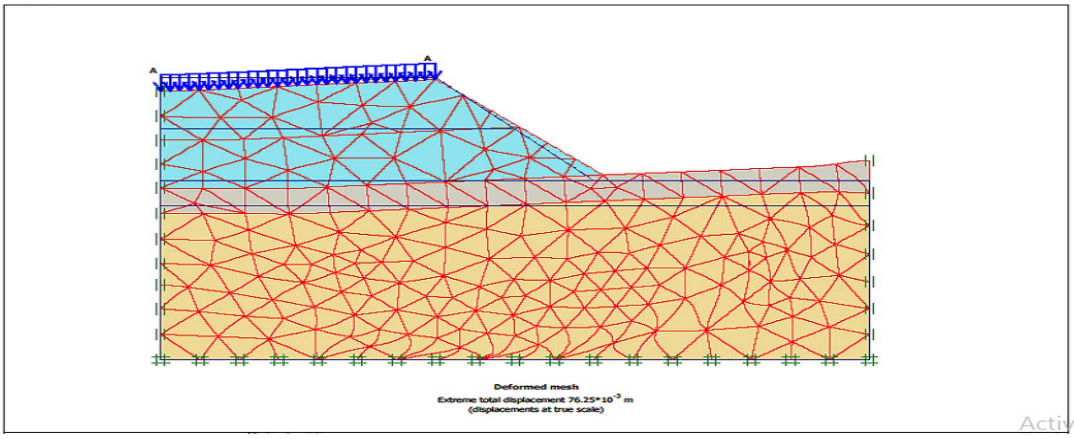

(b) Deformation mesh

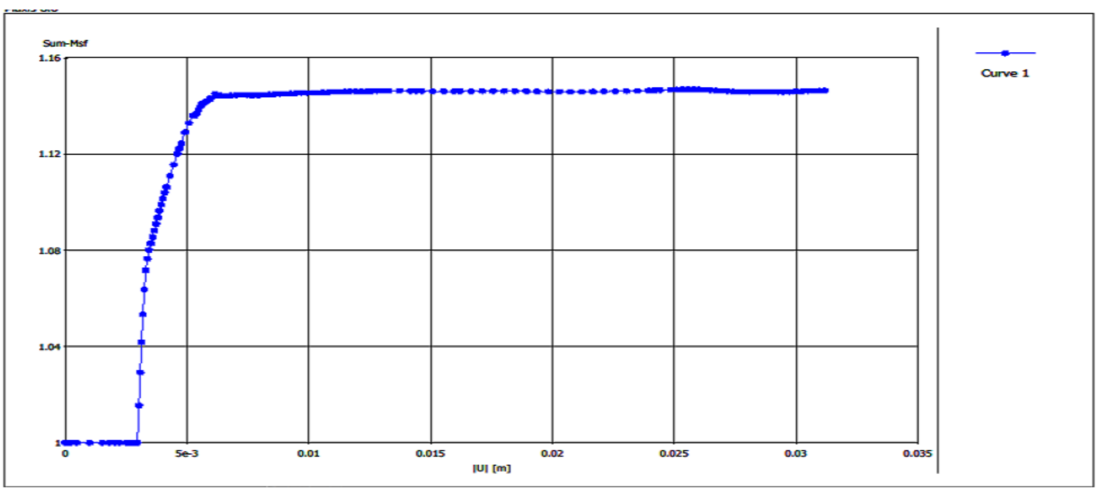

(c) Factor of safety

Fig.4.7.Calculation stage, deformed mesh and FOS for NG1 geocell reinforced embankment

NG2 GEOCELL-

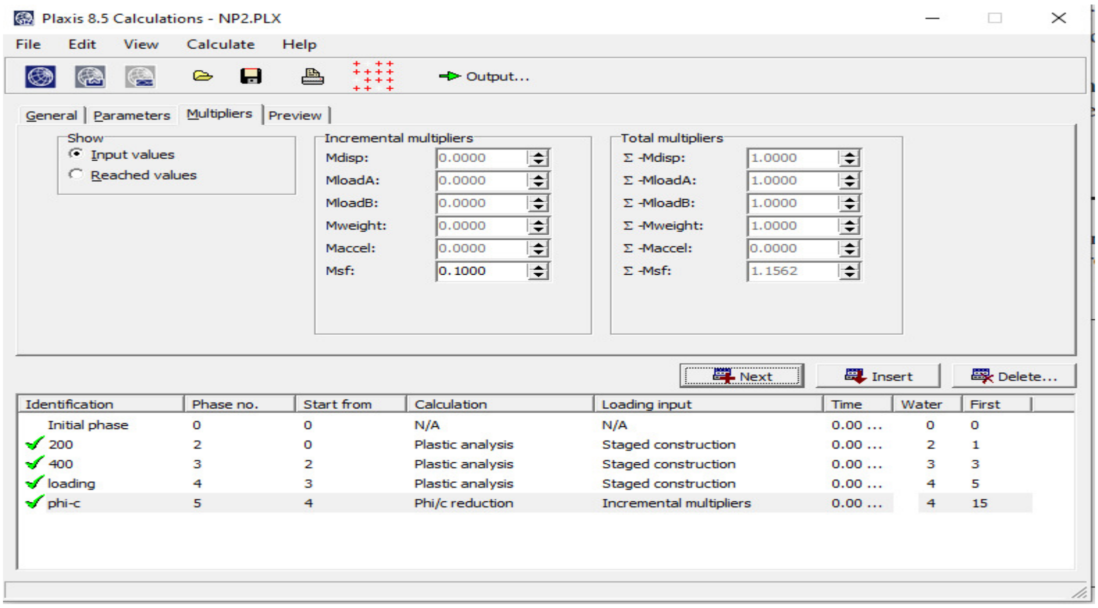

(a) Calculation stage

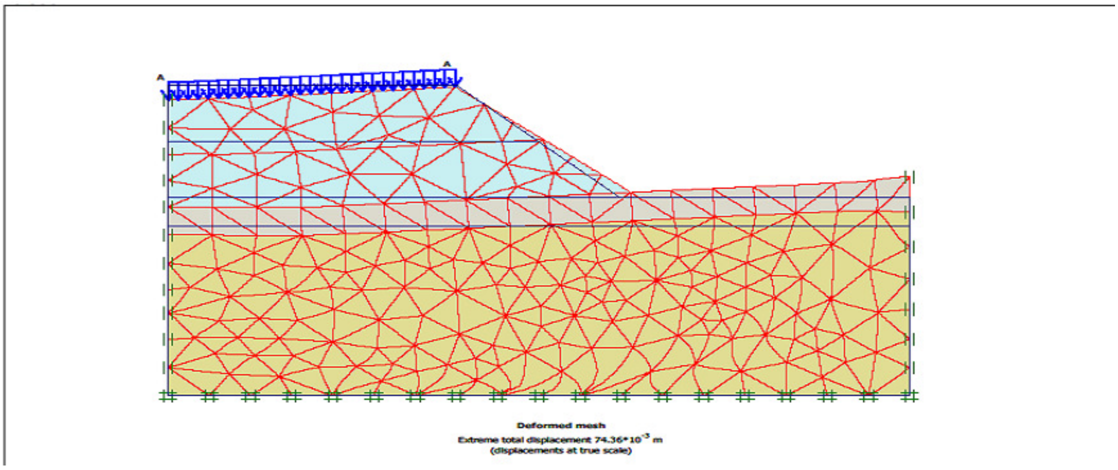

(b) Deformed mesh

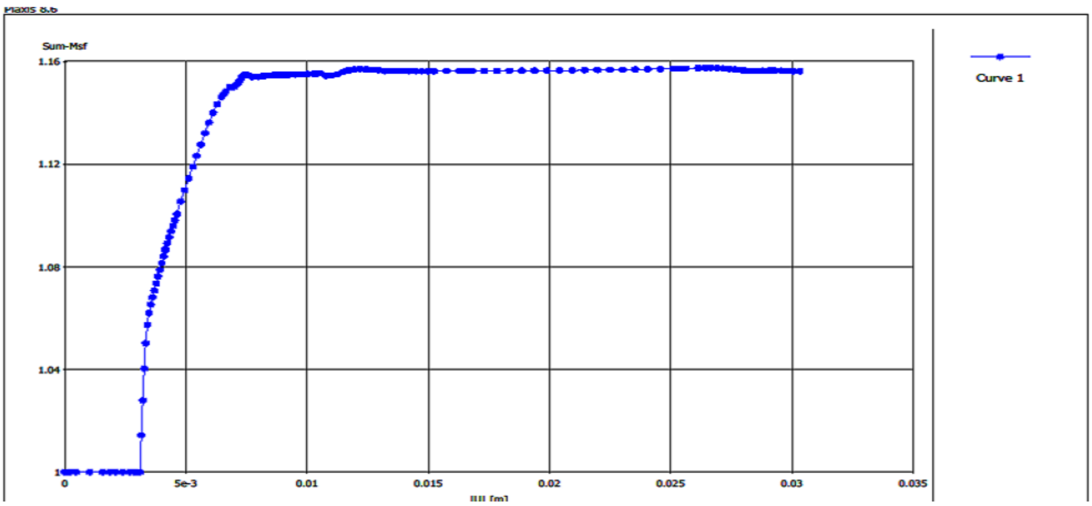

(c) Factor of safety (NG2)

Fig.4.8.Calculation stage, deformed mesh and FOS for NG2 geocell reinforced embankment

The geocells provide cellular confinement to the soil which prevents the horizontal dispersion of soil-filled in geocell openings. The granular soil poses higher shear strength than the cohesive soil. In the case of the unreinforced embankment, the heaving of soil at the base of the embankment is seen in Fig. 4.1(b). While in the case of other types of geocells, no surface heaving occurred. Although at the boundary of the model, an upward displacement is seen, this may be due to the conversion of the geocell mattress into an equivalent soil layer without providing proper anchorage of the geocells to stay intact. During the application of geocells in field, proper anchorage, to keep the geocells intact at its place, is provided, which could not be simulated in the model. The surcharge load to achieve the FOS of 1.15 for all the types of geocells has been shown in Table.4.1.

Table.4.1. Surcharge load to achieve FOS of 1.15

Type of geocell	Surcharge load (kPa)
Unreinforced	46
UG01	75
BG01	69
BG015	78
BG02	86
BG01 (clay)	50
NG1	58
NG2	63

When the load is applied in a geocell reinforced soil, the soil underneath the loading area begins to get pushed downwards after full mobilization of the friction force generated at the interface of infill soil-geocell walls. From the deformation meshes of BG geogrids of height 100mm (Fig.4.3 (b), 150 mm(Fig.4.4(b)) and 200mm(Fig.4.5.(c))-it can be seen that more the height of the geocells, lesser is the deformation of the soil. The contact area of the infill material of the geocell pockets with the walls of the geocells increases leading to greater mobilization of restraining forces or membrane stresses. This increases the friction resistance of soil and decreases the vertical settlement of the soil. When the height of the geocell layer is increased, this downward movement of soil gets completely arrested at a certain stage and the soil-geocell layer starts acting as a single composite unit. In addition to this, the moment of inertia increases when the height of the geocell is increased. Therefore, the bending and shear rigidity of the soil-geocell layer increases because of which even after the shear failure of soil inside the geocell pockets, the geocell layer continues to support the load of the embankment. The provision of geocell decreases the settlement of the soil and distributes the pressure to deeper layers and over a wider area by intercepting the planes of potential failure. When the thickness of the geocell is not enough, the soil does not get enough interlocking and interfacial frictional resistance from the periphery of the geocells and may slip out from the base of the geocell layer. This leads to the lateral spreading of the soil and increased surface heaving.

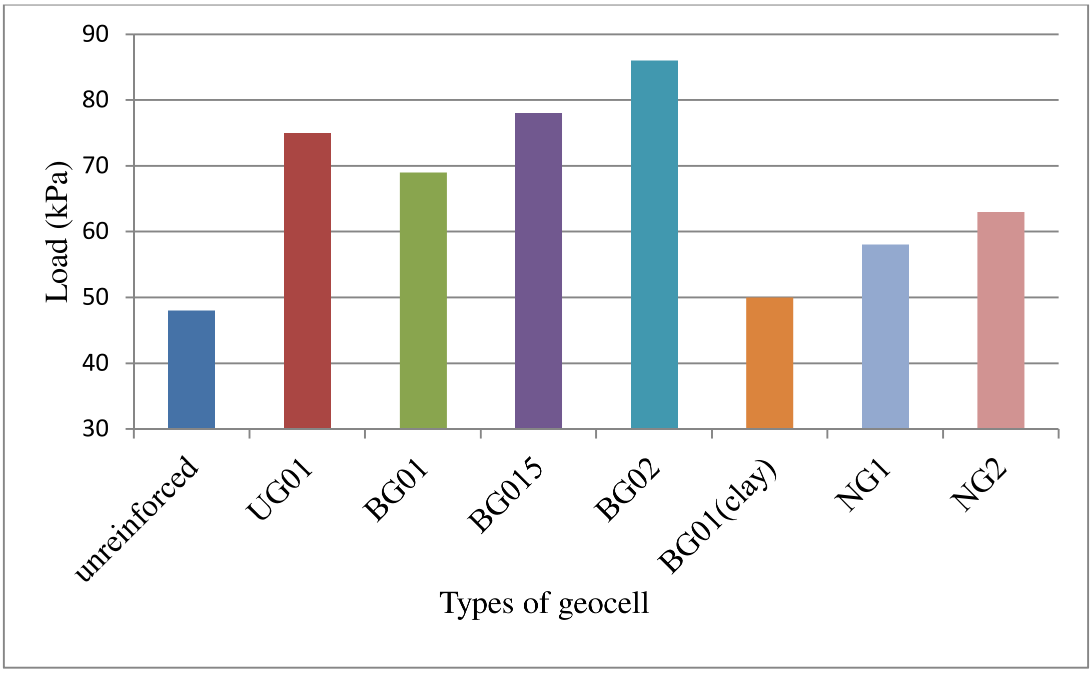

Fig.4.9. Surcharge load value on embankment reinforced with different types of geocells to achieve FOS 1.15

Although, the surcharge load in the case of clay filled geocells showed considerably higher value in comparison with the unreinforced embankment. This means that during the unavailability of good infill material near the sites, easily available soil may be used to fill geocell pockets. The density of the granular soil being more than the fine grained soil, higher frictional force is generated at the interface of soil-geocell walls which prevents downward penetration of the granular soil and provides rigidity to the geocell walls. Also, denser the soil in the geocell pockets, more will be the dilation. This contributes to higher mobilisation of strains in the geocell surface and therefore its enhanced performance.

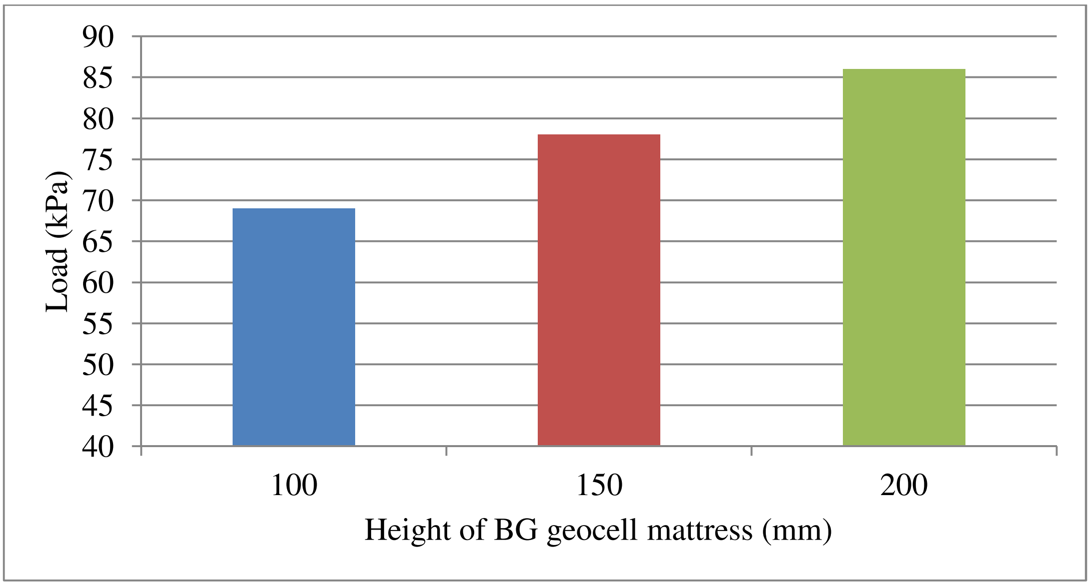

Fig.4.10. Surcharge load value on embankment reinforced with BG geocell of varying depth to achieve FOS 1.15

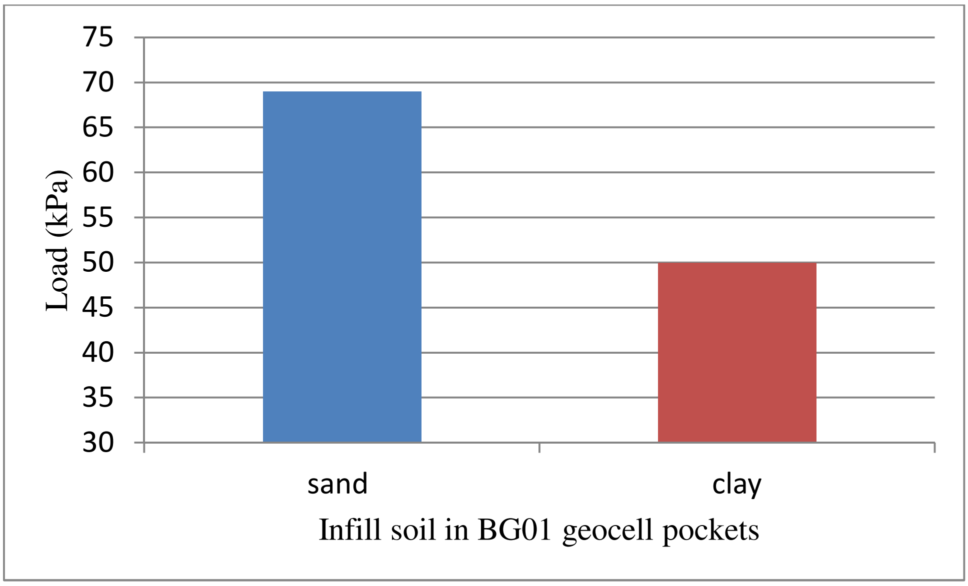

Fig.4.11. Surcharge load value on embankment reinforced with BG01 geocell with sand and clay as infill to achieve FOS 1.15

In the case of BG geocell filled with clayey soil, there is an abrupt deformation at the base of the embankment. This may be due to the lesser shear strength of clayey soil. In addition to this, it is difficult to compact geocells encapsulated with clayey soil. The load, for the sand-filled geocell, to achieve a factor of safety of 1.15 is 1.4 times that of the clayey filled geocells.

For designing problems of embankment, if the field data is available- properties of embankment fill soil and foundation soil, one can determine the type of geocell that would be suitable for the embankment construction by trials run on the software as explained below.

Consider embankment soil- sand- to fill the geocell mattress.

The first step should be to assume certain height of the geocell mattress and then replicating it with that of soil in terms of its strength. Let the height of the geocell mattress be 1m.

Assume a layer of soil, in place of geocell mattress, of 1m and assign certain cohesion value to it, say x and then find the factor of safety by PLAXIS. The angle of friction will be same as that of the infill soil in geocells.

If the obtained factor of safety is not as desired, change the cohesive value of the geocell layer.

If the factor of safety comes out to be the required value, following steps are followed.

The cohesion value due to geocells alone (C_g) can be obtained as follows:

$$C_g = C_{sg} - C_s \qquad (5)$$

Where C_{sg} is the cohesive strength of the geocell when filled with soil

C_s is the strength of the soil with which geocell mattress is filled

The angle of internal friction of the soil is $\emptyset$. the coefficient of passive earth pressure (K_p) is given by:

$$K_p = \frac{1+sin\emptyset}{1-sin\emptyset} \qquad (6)$$

From eq (1), obtain the value of $\Delta\ \sigma_3$ by substituting the value of C_g andK_p.

Consider the following assumptions:

Axial strain in geocell wall (ε_a) = 5%

Initial diameter of cells of geocll mattress (d_0)= 1m

Substitute the values in eq (2) and obtain the value of M.

$$\Delta \sigma_3 = \frac{2M}{d_0} \frac{1-\sqrt{1-\varepsilon_a}}{1-\varepsilon_a} \tag{8}$$

The geocells having secant modulus (M) greater than the calculated value of M can be provided at the base of the embankment to obtain the desired factor of safety.

DESIGN EXAMPLE

To construct an embankment, having safety factor 1.2, determine the type and geometry of the geocell suitable for the construction. The height of the embankment is 4m.

Table.4.2. Data for the design of embankment

Description	Properties	Value
Foundation soil-Clay	Undrained shear strength	20KPa
	Density	15KPa
Embankment soil-Sand	Angle of internal friction	35°
	Cohesion	12KPa
	Density	20KPa
Surcharge load		50KPa

Obtain the geometry of the problem in PLAXIS. Assume the depth of the geocell layer is 1m. The angle of friction of the geocell infill soil will be the same as of infill soil, 35°.

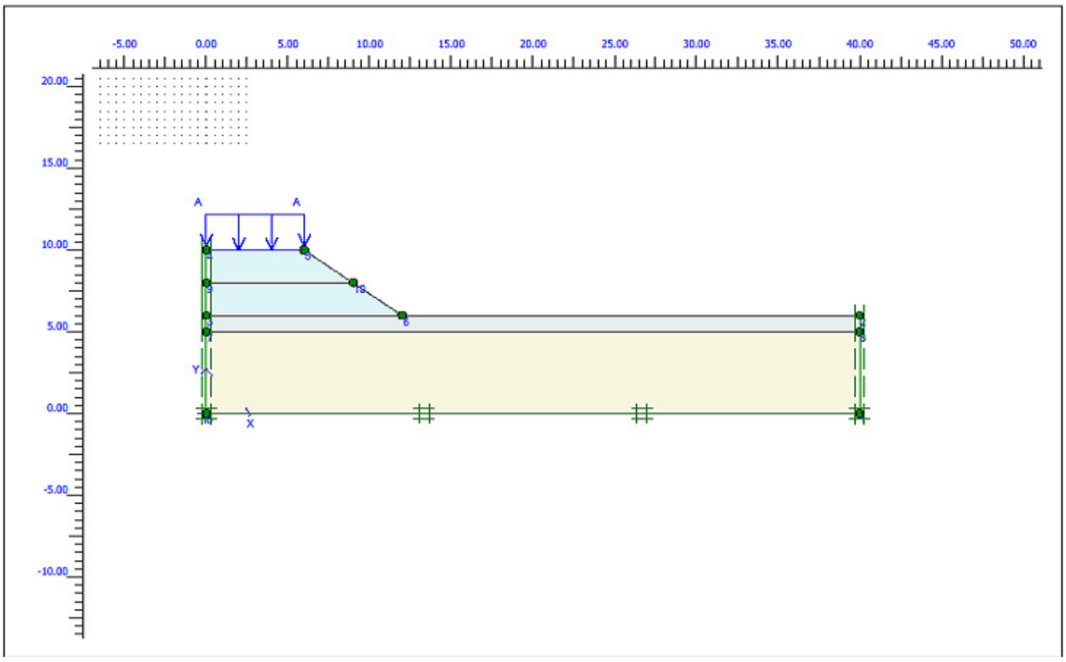

Fig. 4.12. Embankment model

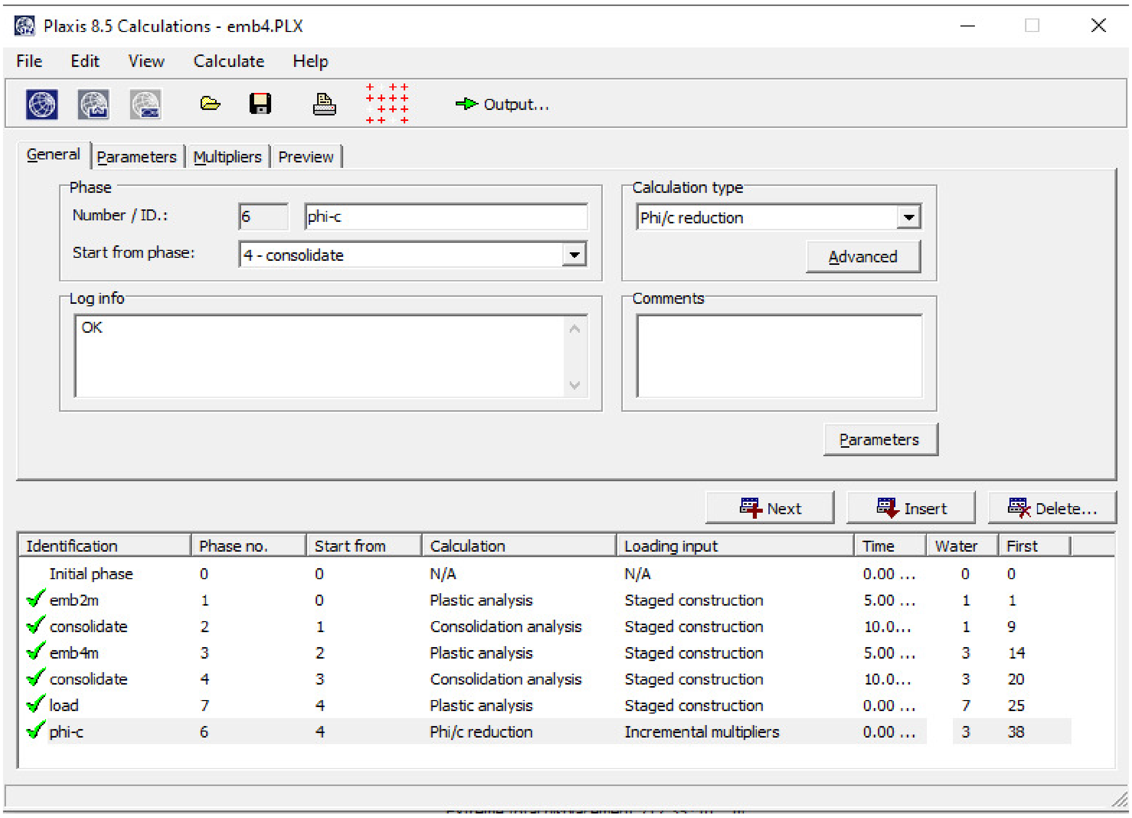

Fig. 4.13.Calculation phase in embankment design

The factor of safety of the embankment is obtained as 1.2 as shown in the figure below which is the aim of the problem.

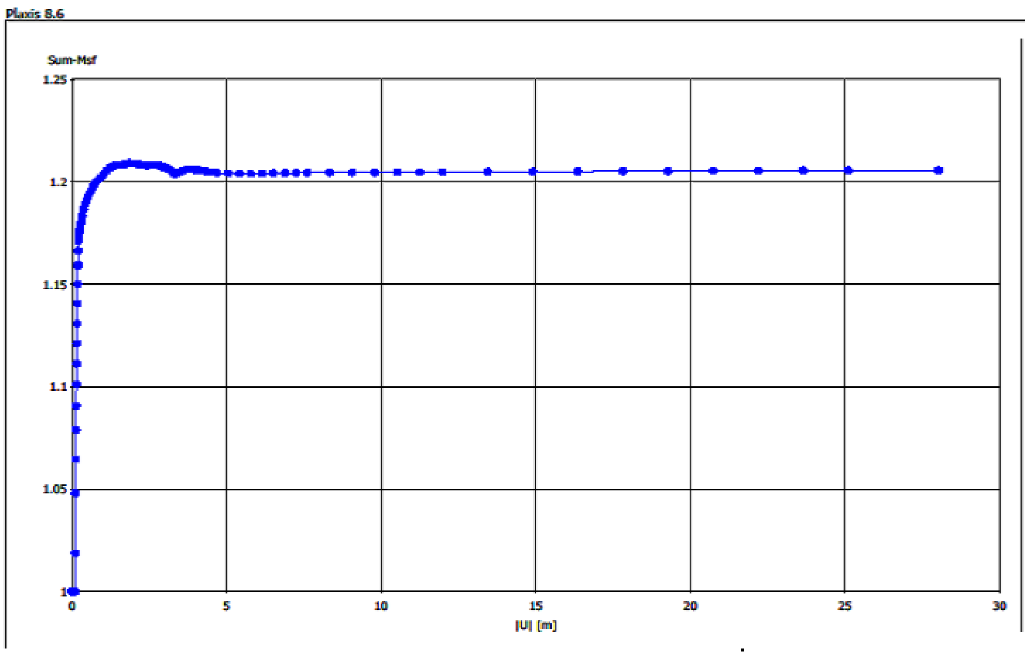

Fig. 4.14. Factor of safety for embankment

Using Eq (5), the cohesion value due to geocells alone (C_g):

$$C_g = C_{sg} - C_s$$

$$C_g = 22 - 12$$

$$C_g = 10\text{KPa}$$

The coefficient of passive earth pressure (K_p) is obtained by Eq. (6):

$$K_p = \frac{1 + sin\emptyset}{1 - sin\emptyset}$$

$$K_p = \frac{1 + sin35}{1 - sin35}$$

$$K_p = 3.69$$

From eq (1), obtain the value of $\triangle\, \sigma_3$ by substituting the value of C_g and K_p as:

$$C_g = \frac{\triangle\, \sigma_3}{2}\sqrt{K_p}$$

$$10 = \frac{\triangle\, \sigma_3}{2}\sqrt{3.690}$$

$$\triangle\, \sigma_3 = 10.411\ KPa$$

Now, make the following assumptions:

Axial strain in geocell wall (ε_a) = 5%

Initial diameter of cells of geocell mattress (d_0) = 1m

Substitute the values in eq (8) and obtain the value of M.

$$\triangle\, \sigma_3 = \frac{2M}{d_0}\frac{1 - \sqrt{1 - \varepsilon_a}}{1 - \varepsilon_a} = \frac{2M\, \varepsilon_c}{d_e}\frac{1 - \sqrt{1 - \varepsilon_a}}{1 - \varepsilon_a}$$

$$\triangle\, \sigma_3 = \frac{2M}{d_0}\frac{1 - \sqrt{1 - \varepsilon_a}}{1 - \varepsilon_a}$$

$$10.411 = \frac{2M}{1}\frac{1 - \sqrt{1 - 0.05}}{1 - 0.05}$$

$$M = 195.304\ \text{kN/m}$$

From Table 3.1, the UG geocell has a secant modulus of 200 kN/m. Therefore, it is suitable for embankment construction to obtain the factor of safety of 1.2 for the given example.

Table.4.3. Parameters for design of the embankment

DESCRIPTION	PROPERTIES	VALUE
Geocell	Height	1m
	Internal diameter	1m
	Secant modulus calculated	195 kN/m
UG geocell	Secant modulus	200 kN/m

CHAPTER 5

CONCLUSIONS AND RECOMMENDATION FOR FUTURE WORK

The experimental results of the geocell reinforced embankment have been carried out in PLAXIS 2D. The geocell reinforced layer of soil was simulated as equivalent soil layer by empirical equations. The characteristics of geocells, height and secant modulus of geocell, and type of soil used for filling the geocell pockets are sensitive criteria for determining the performance of geocell reinforced embankment. The geocell encased with sand can carry a surcharge load of up to 1.72 times that of surcharge load by geocell encased with clay. Geocell pockets filled with sand showed greater load-bearing capacity and lesser settlement than the geocell pockets filled with clay due to higher interlocking and frictional resistance in the sand. The geocell mattress of greater thickness showed better performance. The load-bearing capacity increased from 69 kPa to 86 kPa as the height of BG geocell was increased from 100 mm to 200mm. This is due to the greater surface area available for interfacial frictional resistance between infill material in cells and the wall of the cells.

Geocells, in comparison to other geosynthetics, provide a 3-D structure for soil confinement. Many model studies on small scales have been carried out to study geocells effects in geotechnical engineering. Though, full-scale tests for appropriate scaling have to be done to ascertain the model results in the field. There can be more realistic numerical simulations to study the stress and strain variation of geocell reinforced soils.

REFERENCES

[1] Avesani Neto, J. O., Bueno, B. S. and Futai, M. M. (2013) "A bearing capacity calculation method for soil reinforced with a geocell", *Geosynthetics International*, Elsevier,Vol.20(3), pp. 129–142.

[2] Bathurst, R. J., and Karpurapu, R. (1993). "Large-scale triaxial compression testing of geocell-reinforced granular soils." *Geotech. Test. J.*, Vol.16 (2), pp 296–303.

[3] Biabani, M. M., Indraratna, B. and Ngo, N. T. (2016) "Modelling of geocell-reinforced subballast subjected to cyclic loading", *Geotextiles and Geomembranes*. Elsevier Ltd, Vol.44(4), pp. 489–503.

[4] Biabani, M. M., Ngo, N. T. and Indraratna, B. (2016) "Performance evaluation of railway subballast stabilised with geocell based on pull-out testing", *Geotextiles and Geomembranes*. Elsevier Ltd,Vol. 44(4), pp. 579–591.

[5] Dash, S. K. (2012) "Effect of geocell type on load-carrying mechanisms of geocell-reinforced sand foundations", *International Journal of Geomechanics*,Elsevier,Vol.56(2),pp.12-15

[6] Dash, S. K. and Bora, M. C. (2013) "Improved performance of soft clay foundations using stone columns and geocell-sand mattress", *Geotextiles and Geomembranes*. Elsevier Ltd, 41, pp. 26–35.

[7] Dash, S. K., Krishnaswamy, N. R. and Rajagopal, K. (2001) "Bearing capacity of strip footings supported on", *Geotextiles and Geomembranes*, Elsevier,Vol.19(4), pp. 235–256.

[8] Dash, S. K., Rajagopal, K. and Krishnaswamy, N. R. (2004) "Performance of different geosynthetic reinforcement materials in sand foundations", *Geosynthetics International*,Elsevier,Vol.14(7),pp.34-37.

[9] Dash, S. K., Rajagopal, K. and Krishnaswamy, N. R. (2007) "Behaviour of geocell-reinforced sand beds under strip loading", *Canadian Geotechnical Journal*, Vol.44(7), pp. 905–916.

[10] Dash, S. K., Sireesh, S. and Sitharam, T. G. (2003) "Model studies on circular footing supported on geocell reinforced sand underlain by soft clay", *Geotextiles and Geomembranes*. Elsevier,Vol.15(5),pp.67-71

[11] Duncan, J. M., and Chang, C. Y. (1970). "Nonlinear analysis of stress and strain in soils." *J. Soil Mech. and Found. Div.*, Vol.96 (5),pp. 1629–1653.

[12] Deventer.V., John S. J. and Wan.S.Y. (2010) "Chemical research and climate change as drivers in the commercial adoption of alkali activated materials", *Waste and Biomass Valorization*, Vol.1(1), pp. 145–155.

[13] George, V. and Marathe, S. (2016) "Stability Analysis of lateritic soil Embankment sub-grade Using plaxis-2D" I*nternational Journal for Research in Civil Engineering*.ASCE,Vol.45(3)pp.23-27.

[14] Han, J. *et al.* (2008) "Behavior of geocell-reinforced sand under a vertical load", *Transportation Research Record*

[15] Hegde, A. (2017) "Geocell reinforced foundation beds-past findings, present trends and future prospects: A state-of-the-art review", *Construction and Building Materials*.Elsevier,Vol.32(14), pp.98-101.

[16] Hegde, A. M. and Sitharam, T. G. (2015) "Effect of infill materials on the performance of geocell reinforced soft clay beds", *Geomechanics and Geoengineering*, Elsevier.Vol.10(3), pp. 163–173.

[17] Hegde, A. and Sitharam, T. G. (2015) "3-Dimensional numerical modelling of

geocell reinforced sand beds", *Geotextiles and Geomembranes*. Elsevier Ltd, Vol.43(2), pp. 171–181.

[18] Henkel, D. J., and Gilbert, G. C.(1952). "The effect of rubber membranes on the measured triaxial compression strength of clay samples." *Geotechnique*, Elsevier. Vol.3, pp.20–29.

[19] Kumar, S., Sahu, A. K. and Naval, S. (2019) "Performance of Circular Footing on Expansive Soil Bed Reinforced with Geocells of Chevron Pattern", *Civil Engineering Journal*, Vol.5(11), pp. 2333–2348.

[20] Kumawat, N. K. and Tiwari, S. K. (2017) "Bearing capacity of square footing on geocell reinforced fly ash beds", *Materials Today: Proceedings*. Elsevier Ltd, Vol.4(9), pp. 10570–10580.

[21] Lal, D., Sankar, N. and Chandrakaran, S. (2017) "Effect of reinforcement form on the behaviour of coir geotextile reinforced sand beds", *Soils and Foundations*. Japanese Geotechnical Society, Vol.57(2), pp. 227–236.

[22] Latha, G. M., Dash, S. K. and Rajagopal, K. (2009) "Numerical simulation of the behavior of geocell reinforced sand in foundations", *International Journal of Geomechanics*, Elsevier,Vol.9(4), pp. 143–152.

[23] Latha, G. M., Rajagopal, K. and Krishnaswamy, N. R. (2006) "Experimental and theoretical investigations on geocell-supported embankments", *International Journal of Geomechanics*.ASCE,Vol.10(23),pp.19-22.

[24] Leshchinsky, B. and Ling, H. (2013) "Effects of geocell confinement on strength and deformation behavior of gravel", *Journal of Geotechnical and Geoenvironmental Engineering*,Elsevier. Vol.139(2), pp. 340–352.

[25] Leshchinsky, B. and Ling, H. I. (2013) "Numerical modeling of behavior of railway ballasted structure with geocell confinement", *Geotextiles and Geomembranes*. Elsevier Ltd,Vol. 36(3), pp. 33–43.

[26] Madhavi Latha, G. and Rajagopal, K. (2007) "Parametric finite element analyses of geocell-supported embankments", *Canadian Geotechnical Journal*,ELsevier. Vol.44(8), pp. 917–927.

[27] Madhavi Latha, G. and Somwanshi, A. (2009) "Effect of reinforcement form on the bearing capacity of square footings on sand", *Geotextiles and Geomembranes*. Elsevier Ltd, 27(6), pp. 409–422.

[28] Mamatha, K. H. and Dinesh, S. V (2017) "Performance evaluation of geocell-reinforced pavements", *International Journal of Geotechnical Engineering*. Taylor & Francis, 6362(July), pp. 1–10.

[29] Mehdipour, I., Ghazavi, M. and Moayed, R. Z. (2013) "Numerical study on stability analysis of geocell reinforced slopes by considering the bending effect", *Geotextiles and Geomembranes*. Elsevier Ltd,Vol. 37(3), pp. 23–34.

[30] Mehdipour, I., Ghazavi, M. and Moayed, R. Z. (2017) "Stability analysis of geocell-reinforced slopes using the limit equilibrium horizontal slice method", *International Journal of Geomechanics*,Elsevier. Vol.17(9), pp. 1–15.

[31] Rajagopal, K., Krishnaswamy, N. R. and Latha, G. M. (1999) "Behaviour of sand confined with single and multiple geocells", *Geotextiles and Geomembranes.* Elsevier.Vol.18(4),pp.34-38.

[32] Sireesh, S., Sitharam, T. G. and Dash, S. K. (2009) "Bearing capacity of circular footing on geocell-sand mattress overlying clay bed with void", *Geotextiles and Geomembranes*. Elsevier Ltd, Vol.27(2), pp. 89–98.

[33] Sri, P. and Tjandra, D. (2015) "Analysis of geotextile reinforced road embankment using PLAXIS 2D", *Procedia Engineering*. Elsevier B.V., 125, pp. 358–362.

[34] Tafreshi, S. N. M., Khalaj, O. and Dawson, A. R. (2014) "Repeated loading of soil containing granulated rubber and multiple geocell layers", *Geotextiles and Geomembranes*. Elsevier Ltd, Vol.42(1), pp. 25–38

[35] Zhou, H. and Wen, X. (2008) "Model studies on geogrid- or geocell-reinforced sand cushion on soft soil", *Geotextiles and Geomembranes*, Elsevier.Vol.26(3), pp. 231–238.